Symbiotic Ambient Backscatter Systems: Outage Behavior and Ergodic Capacity

Haiyang Ding, *Member*, *IEEE*, Mohamed-Slim Alouini, *Fellow*, *IEEE*, Kewei Xin, Haipeng Li, and Shengzhi Xu

***Abstract*—This paper investigates a symbiotic ambient backscatter communication (AmBC) system, where for the primary system, a source node T1 transmits information to a destination node T2. Whereas for the backscatter system, by riding on T1's signal, backscatter device passively conveys its own information $c(n)$ to T1 and T2 via backscattering. For such, the coexistence outage probability (COP) and ergodic capacity (EC) of the AmBC system are characterized for three cases of coexistence constraints, i.e., (i) both T1 and T2 decode $c(n)$ (Case I), (ii) only T2 decodes $c(n)$ (Case II), and (iii) only T1 decodes $c(n)$ (Case III). It is analytically shown that for sufficiently high transmit signal-to-noise ratio (SNR), the COP obeys the scaling law of $\frac{1}{\sqrt{P_s}}$ (with P_s denoting T1's transmit power) for Cases I and III, whereas its scaling law is determined by $\frac{\log(P_s)}{P_s}$ as well as $\frac{1}{P_s}$ for Case II. In addition, it is shown that the restriction condition of decoding $c(n)$ at T1 results in a dominating term $\frac{1}{\sqrt{P_s}}$ for the COP at high SNR, whereas the restriction condition of decoding $c(n)$ at T2 results in an infinitesimal relative to $\frac{1}{\sqrt{P_s}}$. It is also shown that for different cases, the effects of the T1-T2 channel statistics on the COP are significantly different. However, unlike the metric of COP, for the EC, the impacts of decoding constraints of $c(n)$ gradually disappear at high SNR and the ECs of the backscatter channels for Cases II and III approach respectively toward the counterpart for Case I.**

***Index Terms*—Ambient backscatter communications, symbiotic communications, outage behavior, ergodic capacity.**

I. Introduction

SPECTRUM scarcity and energy efficiency are envisioned as two primary issues for the large-scale deployment of a future Internet of Things (IoT), which is supposed to connect billions of small computing devices embedded in objects and environments such as books, furniture, home appliances, and even implantable medical devices [1]–[4]. To address this, a promising solution, namely, ambient backscatter communications[1], is attracting significant attentions from both academic and industrial communities. For such, by modulating and reflecting the environmental RF signals from ambient TV towers, cellular base stations, and Wi-Fi routers, the information belonging to the backscatter device (BD) is conveyed in a passive and low-power manner, which improves the spectrum efficiency and lowers energy consumption at the BD node.

This work was supported in part by the National Key R&D Program of China under Grant 2018YFE0100500, in part by the National Natural Science Foundation of China under Grant 61871387, in part by the NUDT Research Fund under Grant ZK20-21, and in part by the Natural Science Basic Research Program of Shaanxi under Grant 2021JQ-378. H. Ding, K. Xin, H. Li, and S. Xu are with the Youth Innovation Team of Shaanxi Universities.

H. Ding, K. Xin, H. Li, and S. Xu are with the School of Information and Communications, National University of Defense Technology, Xi'an, 710106, China. (email: dinghy2003@hotmail.com).

M.-S. Alouini is with the Electrical Engineering Program, Computer, Electrical, and Mathematical Science and Engineering (CEMSE) Division, King Abdullah University of Science and Technology (KAUST), Thuwal, Makkah Province, Saudi Arabia (email: slim.alouini@kaust.edu.sa).

[1]Unlike the monostatic and bistatic backscatter communications that employ dedicated RF source as the carrier signal [2], in this work we focus on ambient backscatter communication which utilizes the ambient RF sources, such as TV towers, cellular base stations, and Wi-Fi APs, as carrier signal.

A. Related Works

1) Ambient Backscatter Communications (AmBC): In [5], a seminal AmBC prototype was introduced, which enables connectivity among small computing devices with the aid of environmental RF signals. Then, Parks *et al* presented the first multi-antenna interference cancellation design for AmBC in addition to a novel multiple-access enabled coding method [6]. After that, [7] proposed a high-throughput, sufficient range and low-power AmBC prototype, a.k.a. BackFi, by using ambient WiFi signals, where the range and throughput of the prototype can be further boosted by utilizing multiple antennas at the WiFi AP. The aforementioned works focused on the enabling techniques for the prototype design of AmBC systems although their achievable performance is not fully understood, especially for large-scale deployment. In view of this, [1] employed stochastic geometry to model the large-scale AmBC deployment, and then quantified the coverage and capacity of the considered network. To guarantee non-overlapping subchannels for different backscatter users, the authors of [8] considered shifting the frequencies of backscatter users to avoid co-channel interference (CCI). Then, the authors of [9] studied capacity scaling law of backscatter communication systems with the number of backscatter tags. In addition, [10] and [11] analyzed the capacity and outage performance of an AmBC system and no cooperation was considered between the primary and backscatter systems.

2) Symbiotic AmBC: Unlike [10] and [11], knowing the symbiotic nature of the AmBC systems, a cooperative backscatter mechanism was recently given to tackle the CCI problem from the primary system, where a successive interference cancellation (SIC) algorithm was used to remove the primary signal at the backscatter receiver [12], [13]. Recently, the authors of [14] carried out a resource allocation for a cooperative AmBC system and proposed several symbiotic transmission schemes. Further, [15] characterized the transmission robustness of the cooperative AmBC system proposed by [14] and unveiled the achievable outage performance of several transmission schemes at high signal-to-noise ratio (SNR). In [16], the authors studied the performance of an AmBC system which rides over a non-orthogonal multiple access (NOMA) downlink, and proposed the optimal setup to maximize the ergodic capacity of the AmBC system. [17] further proposed the backscatter cooperation (BC) scheme for NOMA downlinks, where the two end-users cooperate with each other by backscattering surplus power of the received downlink signals. In addition, [18] considered a NOMA uplink scenario, where a delay-sensitive nonenergy-constrained IoT device and multiple delay-tolerant energy-constrained devices communicate with the same access point. The authors of [19] studied a symbiotic AmBC system, where along with the ambient primary transmission from a MU to an AP, a BD node passively conveys its own information to the MU via the ambient carrier emitted by MU. For such, a MAC-layer analysis of the false-alarm/detection probability at AP and a physical-layer outage analysis of the backscatter link $BD \rightarrow MU$ and the primary link $MU \rightarrow AP$ were respectively carried out. In [20], the

authors analyzed the effect of the tag sensitivity on the capacity of a symbiotic AmBC system, where an energy harvesting (EH) and then backscattering mechanism was adopted at the BD node. In [21], the authors considered a three-node symbiotic radio (SR) system, where a secondary transmitter (STx) transmits messages by modulating its information over the radio frequency (RF) signals received from a primary transmitter (PTx). Based on this system model, a maximum-likelihood (ML) detector was used to perform a joint detection of the primary/secondary signals at the destination and the BER performance for the primary and secondary transmissions was then developed, respectively. In [22], the base station (BS) transmits information to two cellular users based on NOMA protocol, while a BD backscatters its own signal by riding on the BS's signal to the two cellular users. In particular, when the BD backscatters its information only to the near cellular user, the backscatter-NOMA system degenerates into a symbiotic radio (SR) system. For such, the authors derived the outage probability, ergodic rate, diversity order and the scaling slope of the ergodic rate for primary link as well as for the backscatter link within the backscatter-NOMA and SR systems, respectively. In [23], the authors developed the ergodic rates of the primary link as well as the secondary/backscatter link of a cooperative ambient backscatter system which is composed of a multi-antenna RF source, a single-antenna backscatter transmitter and a multi-antenna cooperative receiver that aims to decode the signals from the RF source and the backscatter transmitter. Particularly, transmit beamforming is deployed at the RF source and multi-antenna combining is utilized at the cooperative receiver.

B. Motivations and Contributions

It is noteworthy that in the forgoing works, the transmission robustness of the symbiotic AmBC system has been studied either for the backscatter system that rides on the environmental RF carrier [10], [15], [22], [23] or for the primary system that emitting the RF carrier [15], [22], [23]. *Although the primary system and the backscatter system co-exist as a whole in a symbiotic manner, the co-existing capability for the whole symbiotic AmBC system has not been well understood yet. In particular, the coexistence outage probability and the ergodic capacity of the backscatter links is not clear under the symbiotic constraints.* Therefore, the motivations of this work are twofold. On one hand, for the considered symbiotic AmBC systems, along with the primary transmission from T1 to T2, the backscatter (secondary) transmitter BD employs the primary signal $s(n)$ from T1 as a carrier to passively convey its own signal $c(n)$ to T2 and/or to T1. For such a symbiotic AmBC system, we first need to characterize its coexistence capability, where we use the metric of coexistence outage probability, i.e., COP. Specifically, a coexistence outage event occurs when either the primary transmission from T1 to T2, or the backscatter transmission from BD to T1 and/or from BD to T2 is not successful. Further, we need to depict the scaling law of the coexistence capability with respect to the key system parameters. It is noteworthy that whether the primary transmission and the backscatter transmission can coexist as a whole relies on if the backscatter receiver T2 and T1 can decode $c(n)$ successfully. Therefore, we are curious to know the impacts of decoding constraints at T2 and/or at T1 on the coexistence capability of the symbiotic AmBC systems. According to the specific decoding requirements/possibilities, we have to consider three possible cases, which include Case I: both T1 and T2 are required to decode $c(n)$, Case II: only T2 is required to decode $c(n)$, and Case III: only T1 is required to decode $c(n)$. By comparing the COP difference between Case I and the other two cases, we are able to determine the specific impact of the individual decoding operation of $c(n)$ at T2 or at T1 on the COP of the whole symbiotic AmBC system.

On the other hand, the decoding requirements of the three cases mentioned above establish the coexistence constraints for one specified backscatter link. For example, in order to satisfy the coexistence constraints of Case I, the ergodic capacity (EC) of the backscatter link from BD to T2 would be affected by the backscatter link from BD to T1 (i.e., the decoding operation of $c(n)$ at T1), and vice versa. As thus, we need to characterize this impact by analyzing the EC differences of the backscatter links for the aforementioned three cases. In particular, we attempt to determine the impact of the individual decoding operation of $c(n)$ at T2 or at T1 on the EC of the specified backscatter links.

The main contributions of our work can be summarized as follows:
(i) A symbiotic AmBC framework is firstly established, where a primary transceiver T1 conveys information $s(n)$ to a primary receiver T2 via a direct link. Meanwhile, a backscatter device (BD) passively modulates its own information $c(n)$ on the incidence signal from T1 and then backscatters the resulting signal toward T1 and T2. At T2, the primary signal $s(n)$ and the backscattered signal $c(n)$ are recovered via the SIC procedure. At T1, the backscattered signal $c(n)$ is decoded by cancelling its own self-interference signal $s(n)$. In particular, we consider three cases for the system model. For Case I, both T1 and T2 are required to decode $c(n)$. For Case II, only T2 is required to decode $c(n)$, whereas for Case III, only T1 is required to decode $c(n)$. This model depicts a primary transmission from T1 to T2 along with an AmBC transmission from BD to T1 and from BD to T2, where the impacts of decoding operation of $c(n)$ are examined for the above three cases.
(ii) The coexistence capability of the symbiotic AmBC system is measured in terms of coexistence outage probability and our analysis shows that at high SNR, the coexistence outage behavior scales as $\frac{1}{\sqrt{P_s}}$ for Cases I and III, with P_s denoting the transmit power at source. In contrast, for Case II, the scaling law of outage behavior is jointly dominated by $\frac{1}{P_s}$ and $\frac{\log(P_s)}{P_s}$ at high SNR. In addition, the impacts of the restriction conditions of decoding $c(n)$ at T1 and T2 on the coexistence outage probability are characterized, which shows that the restriction condition of decoding $c(n)$ at T1 leads to a dominating term $\frac{1}{\sqrt{P_s}}$ for the coexistence outage probability at high SNR, whereas the restriction condition of decoding $c(n)$ at T2 gradually loses impacts on the coexistence outage probability at high SNR in comparison with that of decoding $c(n)$ at T1.
(iii) Our analytical results show that for the above three cases, the slope of the ergodic capacity of the backscatter channels with respect to the transmit SNR preserves $\frac{1}{\ln(2)}$ at high SNR. Meanwhile, unlike the metric of coexistence outage probability, the impacts of decoding operation of $c(n)$ at T1 or T2 on the ergodic capacity of the backscatter channels gradually disappears in the high SNR regions. In addition, with the improvement of the channel quality within the symbiotic AmBC system, the ergodic capacity gap between the backscatter links BD-T1 and BD-T2 gradually narrows.

Before proceeding to the next section, Table I shows a table which lists the symbols and their definitions used throughout this paper.

TABLE I: Symbol Descriptions

Symbols	Descriptions
λ_{1B}, λ_{2B}, λ_{12}	Average channel power gains
α	Reflection coefficient
η	Backscatter efficiency
$s(n)$	Primary symbol
$c(n)$	Backscatter symbol
P_s	Transmit power at T1
τ_0	SNR threshold to decode $c(n)$
τ_p	SINR threshold to decode $s(n)$
$y_{T_1}(n)$	n-th received signal at T1
$y_{T_2}(n)$	n-th received signal at T2
$\gamma_{T_2,s}(n)$	Received SINR at T2 to decode $s(n)$
$\gamma_{T_2,c}(n)$	Received SNR at T2 to decode $c(n)$
$\gamma_{T_1,c}(n)$	Received SNR at T1 to decode $c(n)$

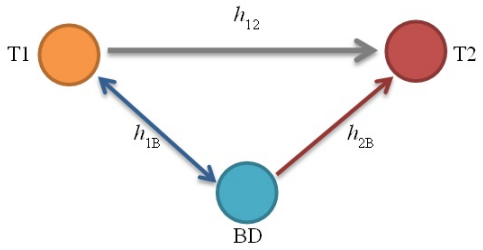

Fig. 1: System model of the considered symbiotic AmBC system.

II. System Model

A. System and Channel Model

As shown by Fig. 1, we consider a symbiotic ambient backscatter communication system, which is composed of a primary system and a backscatter system. For the primary system, the end-source T1 communicates with T2. For the backscatter system, in addition to acquiring the information from T1, T2 also intends to attain information backscattered by BD. Whereas for T1, it also tries to decode the signal backscattered by BD. Without loss of generality, we assume a quasi-static flat Rayleigh fading channel such that the channel power gains conform to exponential distribution with probability density functions (PDF) given by $f_{|h_l|^2}(x) = e^{-\frac{x}{\lambda_l}}/\lambda_l$, where $h_l\,(l \in \{12, 1\mathrm{B}, 2\mathrm{B}\})$ denotes the channel coefficient (of the links T1↔T2, T1↔BD, and T2↔BD, respectively). Herein, the channel reciprocity is assumed and we have $h_{12} = h_{21}, h_{1B} = h_{B1}$, and $h_{2B} = h_{B2}$.

B. Signal Transmission Model

In what follows, the signal transmission process is introduced. First of all, the received signal at T2 can be expressed as

$$y_{T_2}(n) = \sqrt{P_s}h_{12}s(n) + \sqrt{\alpha\eta P_s}h_{1B}h_{2B}c(n)\,s(n) + u_2(n), \tag{1}$$

where $s(n)$ is the signal transmitted by T1, and P_s denotes the transmit power at T1. α and η represent the normalized reflection coefficient and the backscatter efficiency at BD. $c(n)$ denotes the n-th symbol transmitted by BD, and $u_2(n)$ is the normalized additive white Gaussian noise (AWGN) at T2. In particular, $s(n)$ and $c(n)$ are zero mean circular symmetric complex symbols with normalized variance. Note that the second term in (1) indicates the backscattered signal from BD. On the other hand, the backscattered signal from BD is also received[2] by T1, which can be given by

$$y_{T_1}(n) = \sqrt{\alpha\eta P_s}h_{1B}h_{1B}s(n)\,c(n) + u_1(n), \tag{2}$$

where $u_1(n)$ denotes the normalized AWGN at T1. Based on the above results, the received signal-to-interference-plus-noise ratio (SINR) at T2 to decode $s(n)$ is given by

$$\gamma_{T_2,s} = \frac{P_s|h_{12}|^2}{\alpha\eta P_s|h_{1B}|^2|h_{2B}|^2 + 1}. \tag{3}$$

Denoting the SINR threshold to decode $s(n)$ at T2 as τ_p, we assume that T2 decodes $s(n)$ and $c(n)$ by utilizing SIC. Therefore, if $\gamma_{T_2,s} \geq \tau_p$, $s(n)$ can be recovered such that the SNR to decode $c(n)$ at T2 can be expressed as

$$\gamma_{T_2,c} = \alpha\eta P_s|h_{1B}|^2|h_{2B}|^2. \tag{4}$$

At T1, the backscattered signal $c(n)$ is decoded by cancelling its own self-interference signal $s(n)$ such that the received SNR at T1 is given as

$$\gamma_{T_1,c} = \alpha\eta P_s|h_{1B}|^4. \tag{5}$$

As shown by Figure 2, along with the ambient primary transmission from T1 to T2, there are two possible backscatter transmission streams which respectively complete the passive backscatter transmission from BD to T2 and from BD to T1. Specifically, each backscatter frame (either from BD to T2 or from BD to T1) is composed of two parts, i.e., the preamble part and the data transmission part. Similar to [5] and [29], the preamble part consists of the 0/1 wakeup signals, timing signals and the training signals, whereas the data transmission part consists of the data bits. Without loss of generality, we assume the time duration of the data transmission part is much longer than that of the preamble part such that the time

[2]The channel state information (CSI) of loop-interference channel is supposed to be available at T1 to cancel its self-interference signal $s(n)$ such that $c(n)$ can be decoded at T1 for Cases I and III. This can be performed by transmitting pilot signaling by T1 and then estimating the loop-interference channel as in [24], [25], [26]. In this case, a self-interference-free assumption can be made as in [27] and [28].

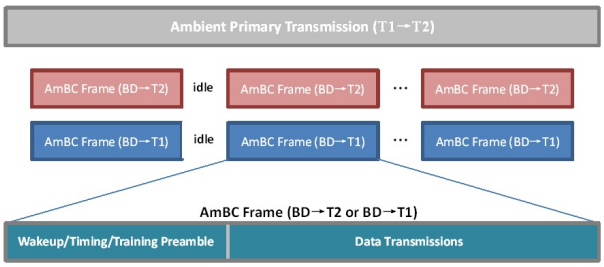

Fig. 2: Frame structure of the AmBC system.

duration of the latter can be safely omitted in comparison with that of the former one. In particular, our theoretical analysis of COP/EC will focus on the data transmission part, as in [14] and [15]. By default, the BD node is in a sleep mode to save energy if it has no data to transmit. Once it has enough data to transmit, the BD's backscatter transmission is activated [5], [29]. In addition, the length of the AmBC frame from BD to T2 and from BD to T1 is exactly the same since the backscattered signal $c(n)$ is emitted by the same BD node.

C. System Setup and Applications

For the considered system model, along with the ambient primary transmission from T1 to T2, we focus on three possible cases for the backscatter transmission from BD to T1 and/or to T2, which include Case I: both T1 and T2 decode $c(n)$, Case II: only T2 decodes $c(n)$, and Case III: only T1 decodes $c(n)$.

The proposed three scenarios may find applications in smart home. For instance, both BS (i.e., T1) and MS (i.e., T2) may need to acquire the status data of a home appliance such as the temperature setup of a refrigerator (i.e., BD), and the data acquisition process can be modeled by Case I in this work. On the other hand, when only MS or BS has the need to attain the status data of the refrigerator, this corresponds to Cases II or III. In general, for the proposed system model, the T1-BD-T1 link depicts the monostatic backscatter channel, whereas the T1-BD-T2 link models the ambient backscatter channel in practice. Notably, the proposed symbiotic AmBC framework has the advantage of a double exploitation of the same spectrum of the primary system to transmit additional backscatter information, which makes it very appealing to solve the spectrum scarcity problem in the next-generation IoT networks. For the above three application scenarios, in the following sections we'll analyze the coexistence capability in terms of the coexistence outage probability of the symbiotic AmBC system as well as the ergodic capacity of the backscatter channels under the constraint of decoding $c(n)$ at T1 and/or T2.

III. Coexistence Probability and Outage Analysis

In this section, we characterize the coexistence capability of the primary system and the backscatter systems in terms of coexistence outage probability (COP) for three possible cases, i.e., Case I: both T1 and T2 decode $c(n)$, Case II: only T2 decodes $c(n)$, and Case III: only T1 decodes $c(n)$.

A. Both T1 and T2 Decode $c(n)$

We define τ_0 as the SNR threshold to recover $c(n)$. In other words, to ensure that T1 and T2 decode BD's signal $c(n)$ successfully, inequalities $\gamma_{T_1,c} \geq \tau_0$ and $\gamma_{T_2,c} \geq \tau_0$ have to be satisfied. Therefore, the condition to successfully decode $s(n)$ and $c(n)$ at T2 can be expressed as $\left\{\frac{P_s|h_{12}|^2}{\alpha\eta P_s|h_{1B}|^2|h_{2B}|^2+1} \geq \tau_p, \alpha\eta P_s|h_{1B}|^2|h_{2B}|^2 \geq \tau_0\right\}$, which can be equivalently written as

$$\left\{\frac{\tau_0}{\eta P_s|h_{1B}|^2|h_{2B}|^2} \leq \alpha \leq \frac{\frac{P_s|h_{12}|^2}{\tau_p}-1}{\eta P_s|h_{1B}|^2|h_{2B}|^2}\right\}. \quad (6)$$

In other words, if the normalized reflection coefficient α is adjusted according to (6), T2 would be able to decode $s(n)$ and $c(n)$ successfully. To make this happen, inequalities $\tau_0 \leq \frac{P_s|h_{12}|^2}{\tau_p} - 1$ and $\frac{\tau_0}{\eta P_s|h_{1B}|^2|h_{2B}|^2} \leq 1$ have to hold. On the other hand, for T1, the reflection coefficient α has to be adjusted based on the following condition in order to decode $c(n)$ successfully:

$$\alpha \geq \frac{\tau_0}{\eta P_s|h_{1B}|^4}, \quad (7)$$

in which the condition $\frac{\tau_0}{\eta P_s|h_{1B}|^4} \leq 1$ has to hold to keep a feasible setup of α. To summarize, to make the primary transmission T1→T2 as well as the backscatter transmission BD→T2 and BD→T1 suffer from no information outage, the following conditions have to be satisfied:

$$\frac{\tau_0}{\eta P_s|h_{1B}|^2|h_{2B}|^2} \leq 1, \frac{\tau_0}{\eta P_s|h_{1B}|^4} \leq 1,$$
$$\frac{\tau_0}{\eta P_s|h_{1B}|^4} \leq \frac{\frac{P_s|h_{12}|^2}{\tau_p}-1}{\eta P_s|h_{1B}|^2|h_{2B}|^2}, \tau_0 \leq \frac{P_s|h_{12}|^2}{\tau_p} - 1. \quad (8)$$

Accordingly, the probability of successful coexistence[3] can be written as (9), shown at the top of the next page.

In what follows, we first focus on I_1, which can be reformulated as

$$I_1 = \frac{1}{\lambda_{1B}} e^{-\frac{(\tau_0+1)\tau_p}{\lambda_{12}P_s}} \times \left[\underbrace{\int_{\sqrt{\frac{\tau_0}{\eta P_s}}}^{\infty} e^{-\frac{z_1}{\lambda_{1B}} - \frac{\tau_0}{\lambda_{2B}\eta P_s z_1}} dz_1}_{\xi} - \frac{e^{-\sqrt{\frac{\tau_0}{\eta P_s}}\left(\frac{1}{\lambda_{1B}}+\frac{1}{\lambda_{2B}}\right)}}{\frac{1}{\lambda_{1B}}+\frac{1}{\lambda_{2B}}}\right]. \quad (10)$$

Unfortunately, so far as the authors are concerned, there is no closed-form expression for ξ in (10). To proceed, for sufficiently large P_s, ξ can be asymptotically written as

$$\xi \simeq \sum_{l=0}^{\infty} \frac{\left(-\frac{\tau_0}{\lambda_{2B}\eta P_s}\right)^l}{l!} \int_{\sqrt{\frac{\tau_0}{\eta P_s}}}^{\infty} \left(\frac{1}{z_1}\right)^l e^{-\frac{z_1}{\lambda_{1B}}} dz_1$$
$$\simeq I_{1,0} - \frac{\tau_0}{\lambda_{2B}\eta P_s} I_{1,1} + \frac{\left(\frac{\tau_0}{\lambda_{2B}\eta P_s}\right)^2}{2} I_{1,2}, \quad (11)$$

where we have $I_{1,0} = \lambda_{1B} e^{-\frac{1}{\lambda_{1B}}\sqrt{\frac{\tau_0}{\eta P_s}}}$, $I_{1,1} = -\mathrm{Ei}\left(-\frac{1}{\lambda_{1B}}\sqrt{\frac{\tau_0}{\eta P_s}}\right)$, and $I_{1,2} = \frac{1}{\lambda_{1B}}\mathrm{Ei}\left(-\frac{1}{\lambda_{1B}}\sqrt{\frac{\tau_0}{\eta P_s}}\right) +$

[3]Instead of defining the transmission robustness for the primary and backscatter systems separately [15], [4], [10] and [11], in this work we define the probability of successful coexistence (or equivalently the coexistence outage probability) to evaluate the overall transmission robustness of the whole symbiotic AmBC system.

$$P_{coex}^{T1\to T2}=\underbrace{\Pr\left(|h_{2B}|^2\le|h_{1B}|^2,\frac{\tau_0}{\eta P_s|h_{1B}|^2}\le|h_{2B}|^2,\frac{\tau_0}{|h_{1B}|^2}\le\frac{\frac{P_s|h_{12}|^2}{\tau_p}-1}{|h_{2B}|^2},\tau_0\le\frac{P_s|h_{12}|^2}{\tau_p}-1\right)}_{I_1}$$
$$+\underbrace{\Pr\left(|h_{2B}|^2>|h_{1B}|^2,\frac{\tau_0}{\eta P_s|h_{1B}|^2}\le|h_{1B}|^2,\frac{\tau_0}{|h_{1B}|^2}\le\frac{\frac{P_s|h_{12}|^2}{\tau_p}-1}{|h_{2B}|^2},\tau_0\le\frac{P_s|h_{12}|^2}{\tau_p}-1\right)}_{I_2}. \quad (9)$$

$\sqrt{\frac{\eta P_s}{\tau_0}}e^{-\frac{1}{\lambda_{1B}}\sqrt{\frac{\tau_0}{\eta P_s}}}$. By inserting (11) into (10) and making use of [30, Eq. (8.214.1)], we have

$$I_1\simeq\frac{\lambda_{1B}}{\lambda_{1B}+\lambda_{2B}}+\frac{1}{P_s}\left[\frac{\tau_0}{2\eta}\left(\frac{1}{\lambda_{1B}}\right)^2-\frac{(\tau_0+1)\tau_p\lambda_{1B}}{\lambda_{12}(\lambda_{1B}+\lambda_{2B})}+\right.$$
$$\frac{\tau_0}{\eta\lambda_{1B}\lambda_{2B}}\left(C_{Euler}+\ln\left(\frac{1}{\lambda_{1B}}\sqrt{\frac{\tau_0}{\eta P_s}}\right)\right)$$
$$\left.-\frac{\tau_0\lambda_{2B}}{2\eta(\lambda_{1B}+\lambda_{2B})}\left(\frac{1}{\lambda_{1B}}+\frac{1}{\lambda_{2B}}\right)^2\right], \quad (12)$$

where $C_{Euler}=0.5772156649$ denotes the Euler's constant.

On the other hand, we define $X\triangleq|h_{1B}|^2$, $Y\triangleq|h_{2B}|^2$, and $Z\triangleq|h_{12}|^2$, and rewrite I_2 as

$$I_2=\frac{\lambda_{2B}e^{-\frac{\tau_p(\tau_0+1)}{\lambda_{12}P_s}-\sqrt{\frac{\tau_0}{\eta P_s}}\left(\frac{1}{\lambda_{1B}}+\frac{1}{\lambda_{2B}}\right)}}{\lambda_{1B}+\lambda_{2B}}$$
$$-\frac{e^{-\frac{1}{\lambda_{1B}}\sqrt{\frac{\tau_0}{\eta P_s}}+\frac{1}{\tau_0\lambda_{2B}}\sqrt{\frac{\tau_0}{\eta P_s}}}}{\lambda_{1B}\lambda_{12}}$$
$$\times\underbrace{\int_{\frac{\tau_p(\tau_0+1)}{P_s}}^{\infty}\frac{e^{-\frac{z}{\lambda_{12}}-\sqrt{\frac{\tau_0}{\eta P_s}}\frac{P_sz}{\tau_p\tau_0\lambda_{2B}}}}{\frac{P_sz}{\tau_p\tau_0\lambda_{2B}}+\frac{1}{\lambda_{1B}}-\frac{1}{\tau_0\lambda_{2B}}}dz}_{I_{21}}. \quad (13)$$

With the aid of [30, Eq. (3.352.2)], I_{21} can be asymptotically written as

$$I_{21}\simeq-\frac{\tau_p\tau_0\lambda_{2B}}{P_s}$$
$$\times\left\{C_{Euler}+\ln\left[\frac{\tau_p(\tau_0+1)}{P_s}\left(\frac{1}{\lambda_{12}}+\frac{1}{\tau_p\tau_0\lambda_{2B}}\sqrt{\frac{\tau_0P_s}{\eta}}\right)\right.\right.$$
$$\left.\left.+\frac{\tau_p\tau_0\lambda_{2B}}{P_s}\left(\frac{1}{\lambda_{1B}}-\frac{1}{\tau_0\lambda_{2B}}\right)\left(\frac{1}{\lambda_{12}}+\frac{1}{\tau_p\tau_0\lambda_{2B}}\sqrt{\frac{\tau_0P_s}{\eta}}\right)\right]\right\}. \quad (14)$$

By inserting (14) into (13), I_2 can be asymptotically expressed as

$$I_2\simeq\frac{\lambda_{2B}}{\lambda_{1B}+\lambda_{2B}}$$
$$\times\left\{1+\frac{1}{P_s}\left[-\frac{\tau_p(\tau_0+1)}{\lambda_{12}}+\frac{\tau_0}{2\eta}\left(\frac{1}{\lambda_{1B}}+\frac{1}{\lambda_{2B}}\right)^2\right]\right.$$
$$\left.-\left(\frac{1}{\lambda_{1B}}+\frac{1}{\lambda_{2B}}\right)\sqrt{\frac{\tau_0}{\eta P_s}}\right\}+\frac{\tau_p\tau_0\lambda_{2B}}{\lambda_{1B}\lambda_{12}P_s}$$
$$\times\left\{C_{Euler}+\ln\left[\frac{\tau_0+1}{\tau_0\lambda_{2B}}\sqrt{\frac{\tau_0}{\eta P_s}}+\left(\frac{1}{\lambda_{1B}}-\frac{1}{\tau_0\lambda_{2B}}\right)\sqrt{\frac{\tau_0}{\eta P_s}}\right]\right\}. \quad (15)$$

By summarizing (12) and (15), we can arrive at the following conclusion.

Proposition 1: When both T1 and T2 are required to decode $c(n)$ (Case I), the asymptotic coexistence outage behavior of the symbiotic AmBC system can be written as

$$P_{out}^{T1\to T2}=1-P_{coex}^{T1\to T2}\simeq P_1+P_2+P_3\to P_1, \quad (16)$$

in which we have $P_1=\frac{1}{\lambda_{1B}}\sqrt{\frac{\tau_0}{\eta P_s}}$, $P_2=-\frac{1}{P_s}\frac{\tau_p\tau_0\lambda_{2B}}{\lambda_{1B}\lambda_{12}}\ln\left[\left(\frac{1}{\lambda_{1B}}+\frac{1}{\lambda_{2B}}\right)\sqrt{\frac{\tau_0}{\eta P_s}}\right]-\frac{1}{P_s}\frac{\tau_0}{\eta\lambda_{1B}\lambda_{2B}}\ln\left(\frac{1}{\lambda_{1B}}\sqrt{\frac{\tau_0}{\eta P_s}}\right)$, and $P_3=\frac{1}{P_s}\left\{\frac{\tau_p(\tau_0+1)}{\lambda_{12}}-\frac{\tau_0C_{Euler}}{\lambda_{1B}}\left(\frac{\tau_p\lambda_{2B}}{\lambda_{12}}+\frac{1}{\eta\lambda_{2B}}\right)-\frac{\tau_0}{2\eta}\left(\frac{1}{\lambda_{1B}}\right)^2\right\}$.

Remark 1: It follows from (16) that the asymptotic scaling law of the symbiotic backscatter system is dominated by three kinds of ingredients, i.e., $\frac{1}{\sqrt{P_s}}$, $\frac{1}{P_s}$, and $\frac{1}{P_s}\ln(P_s)$. It will be shown in the numerical results section that all of the three kinds of ingredients are indispensable to accurately depict the high-SNR outage behavior of the symbiotic backscatter systems. However, for sufficiently high SNR, the asymptotic scaling law of the symbiotic backscatter system is dominated by $\frac{1}{\sqrt{P_s}}$.

B. Only T2 Decodes $c(n)$

In this case, to guarantee a successful SIC decoding of $s(n)$ and $c(n)$ at T2, the normalized reflection coefficient has to satisfy $\frac{\tau_0}{\eta P_s|h_{1B}|^2|h_{2B}|^2}\le\alpha\le\frac{\frac{P_s|h_{12}|^2}{\tau_p}-1}{\eta P_s|h_{1B}|^2|h_{2B}|^2}$. Correspondingly, to ensure a feasible setup of α, the following condition has to hold: $\tau_0\le\frac{P_s|h_{12}|^2}{\tau_p}-1$, $\frac{\tau_0}{\eta P_s|h_{1B}|^2|h_{2B}|^2}\le1$. That is to say: the probability of successful coexistence between the backscatter

transmission and primary transmission can be expressed as

$$P_{coex}^{ND-T_1} = \Pr\left(\tau_0 \leq \frac{P_s\left|h_{12}\right|^2}{\tau_p} - 1, \frac{\tau_0}{\eta P_s\left|h_{1B}\right|^2\left|h_{2B}\right|^2} \leq 1\right) = e^{-\frac{\tau_p(\tau_0+1)}{\lambda_{12}P_s}}\left[1 - F_V\left(\frac{\tau_0}{\eta P_s}\right)\right], \quad (17)$$

where $F_V(v) = G_{1,3}^{2,1}\left(\frac{v}{\lambda_{1B}\lambda_{2B}}\middle|\begin{smallmatrix}1\\1,1,0\end{smallmatrix}\right)$ denotes the CDF of $V \triangleq \left|h_{1B}\right|^2\left|h_{2B}\right|^2$, with $G_{1,3}^{2,1}(-|-)$ being the Meijer's G function. To characterize the asymptotic outage behavior of the considered symbiotic ambient backscatter system, we establish the scaling behavior of $F_V\left(\frac{\tau_0}{\eta P_s}\right)$ at high SNR, given in the following Lemma.

Lemma 1: For sufficiently high SNR, $F_V\left(\frac{\tau_0}{\eta P_s}\right)$ can be asymptotically expressed as

$$F_V\left(\frac{\tau_0}{\eta P_s}\right) \simeq \frac{\tau_0}{\eta P_s\lambda_{1B}\lambda_{2B}}\ln\left(\frac{\eta P_s\lambda_{1B}\lambda_{2B}}{4\tau_0}\right) + \frac{\tau_0}{\eta P_s\lambda_{1B}\lambda_{2B}} \propto \frac{\ln(P_s)}{P_s}. \quad (18)$$

Proof: According to [30, Eq. (9.34.3)] and the definition of $F_V(v)$, we have

$$F_V\left(\frac{\tau_0}{\eta P_s}\right) = \frac{2}{\lambda_{21}\lambda_{22}}\int_0^{\frac{\tau_0}{\eta P_s}} K_0\left(2\sqrt{\frac{t}{\lambda_{21}\lambda_{22}}}\right)dt. \quad (19)$$

With the aid of [31, Eq. 9.6.8] and the change of variables, it follows that

$$F_V\left(\frac{\tau_0}{\eta P_s}\right) \simeq -\int_0^{2\sqrt{\frac{\tau_0}{\eta P_s\lambda_{21}\lambda_{22}}}} x\ln(x)dx. \quad (20)$$

Next, invoking the integration by parts and L'Hôpital's rule, we complete the proof. □

Based on Lemma 1, we establish the following proposition.

Proposition 2: When only T2 is required to decode $c(n)$ (Case II), the coexistence outage probability for the symbiotic AmBC system can be asymptotically expressed as

$$P_{out}^{ND-T_1} = 1 - P_{coex}^{ND-T_1} \simeq \frac{\tau_0}{\eta P_s\lambda_{1B}\lambda_{2B}}\ln\left(\frac{\eta P_s\lambda_{1B}\lambda_{2B}}{4\tau_0}\right) + \frac{1}{P_s}\left[\frac{\tau_0}{\eta\lambda_{1B}\lambda_{2B}} + \frac{\tau_p(\tau_0+1)}{\lambda_{12}}\right] \propto \frac{\ln(P_s)}{P_s}. \quad (21)$$

Remark 2: It follows from (21) that the coexistence outage probability scales as $\frac{\ln(P_s)}{P_s}$ at high SNR. In addition, by comparing Proposition 2 with Proposition 1, we notice that the impacts of restriction condition of decoding $c(n)$ at T1 results in a dominating scaling law of $\frac{1}{\sqrt{P_s}}$ for the coexistence outage probability of the whole symbiotic system.

C. Only T1 Decodes $c(n)$

In this case, T2 is only required to decode the signal from T1, i.e., $s(n)$, whereas T1 is required to decode $c(n)$. As a result, to make the primary and the backscatter transmissions coexist with each other, the normalized reflection coefficient α has to satisfy $\frac{\tau_0}{\eta P_s\left|h_{1B}\right|^4} \leq \alpha \leq \frac{\frac{P_s\left|h_{12}\right|^2}{\tau_p}-1}{\eta P_s\left|h_{1B}\right|^2\left|h_{2B}\right|^2}$. Correspondingly, to make the setup of α feasible, inequalities $\frac{\tau_0}{\eta P_s\left|h_{1B}\right|^4} \leq 1$ and $\frac{\tau_0}{\left|h_{1B}\right|^2} \leq \frac{\frac{P_s\left|h_{12}\right|^2}{\tau_p}-1}{\left|h_{2B}\right|^2}$ have to hold. Therefore, the probability of coexistence can be written as

$$P_{coex}^{ND-T_2} = \Pr\left(\frac{\tau_0}{\eta P_s\left|h_{1B}\right|^4} \leq 1, \frac{\tau_0}{\left|h_{1B}\right|^2} \leq \frac{\frac{P_s\left|h_{12}\right|^2}{\tau_p}-1}{\left|h_{2B}\right|^2}\right). \quad (22)$$

By defining $X \triangleq \left|h_{1B}\right|^2$, $Y \triangleq \left|h_{2B}\right|^2$, and $Z \triangleq \left|h_{12}\right|^2$, it follows from [30, Eq. (3.352.2)] that the coexistence outage probability of the symbiotic AmBC system can be characterized in the following proposition.

Proposition 3: When only T1 is required to decode $c(n)$ (Case III), the coexistence outage probability of the symbiotic AmBC system can be asymptotically expressed as

$$P_{out}^{ND-T_2} \simeq \frac{1}{P_s}\left[\frac{\tau_p}{\lambda_{12}} - \frac{1}{2}\left(\frac{1}{\lambda_{1B}}\right)^2\frac{\tau_0}{\eta} - \frac{\tau_p\tau_0\lambda_{2B}}{\lambda_{12}\lambda_{1B}}C_{Euler}\right] + \frac{1}{\lambda_{1B}}\sqrt{\frac{\tau_0}{\eta P_s}} - \frac{\tau_p\tau_0\lambda_{2B}}{\lambda_{12}\lambda_{1B}P_s}\ln\left(\frac{1}{\lambda_{1B}}\sqrt{\frac{\tau_0}{\eta P_s}} + \frac{\tau_p\tau_0\lambda_{2B}}{\lambda_{1B}\lambda_{12}P_s}\right) \to \frac{1}{\lambda_{1B}}\sqrt{\frac{\tau_0}{\eta P_s}}. \quad (23)$$

Remark 3: It follows from Propositions 1-3 that unlike Case II, the asymptotic coexistence outage behavior of the symbiotic AmBC system for Case III is exactly the same with the counterpart for Case I. In other words, the impacts of restriction condition of decoding $c(n)$ at T2 on the coexistence outage probability gradually disappears at high SNR, which is different from the impacts of the restriction condition of decoding $c(n)$ at T1.

IV. Ergodic Capacity

A. Decoding $c(n)$ at T2 and T1

To maximize the rate of the backscatter system, it follows from (6) that the optimal normalized reflection coefficient[4] is $\alpha^* = \min\left[1, \frac{\frac{P_s\left|h_{12}\right|^2}{\tau_p}-1}{\eta P_s\left|h_{1B}\right|^2\left|h_{2B}\right|^2}\right]$. Accordingly, the ergodic capacity of the backscatter transmission at T2 can be written as

$$C_{BC,T_{2,c}} = E\left\{\log_2\left(1 + \gamma_{T_2,c}\big|_{\alpha=\alpha^*}\right)\right\} = E\left\{\log_2\left(1 + \min\left[\eta P_s\left|h_{1B}\right|^2\left|h_{2B}\right|^2, \frac{P_s\left|h_{12}\right|^2}{\tau_p} - 1\right]\right)\right\}, \quad (24)$$

where the expectation operation is taken over (8). As before, we define $X \triangleq \left|h_{1B}\right|^2$, $Y \triangleq \left|h_{2B}\right|^2$, and $Z \triangleq \left|h_{12}\right|^2$, and then reformulate (24) as

$$C_{BC,T_{2,c}} = \underbrace{E_{(8),\ \eta P_s XY \leq \frac{P_s Z}{\tau_p}-1}\left\{\log_2(1+\eta P_s XY)\right\}}_{J_1} + \underbrace{E_{(8),\ \eta P_s XY > \frac{P_s Z}{\tau_p}-1}\left\{\log_2\left(\frac{P_s Z}{\tau_p}\right)\right\}}_{J_2}. \quad (25)$$

[4]To set the optimal reflection coefficient α at BD, global CSI is supposed to be available at BD. This can be achieved by estimating the local CSI h_{1B} and h_{2B} at BD from the pilot signaling sent by T1 and T2, respectively. In addition, the non-local CSI h_{12} can be estimated at T2 from the pilot signaling sent by T1 and then h_{12} will be forwarded from T2 to BD, similar to the approach adopted by [32], [33], and [34].

Next, we first focus on J_1, which can be written as

$$J_1 = \iiint\limits_{(8),\eta P_s xy \le \frac{P_s z}{\tau_p}-1, z \ge \frac{\tau_p}{P_s}} f_X(x) f_Y(y) f_Z(z) \times \log_2(1+\eta P_s xy)\, dxdydz, \quad (26)$$

where the integration region is given by

$$\frac{\tau_0}{\eta P_s xy} \le 1, (27a), \tau_0 \le \frac{P_s z}{\tau_p} - 1, (27b), \frac{\tau_0}{\eta P_s x^2} \le 1, (27c),$$
$$\frac{\tau_0}{\eta P_s x^2} \le \frac{\frac{P_s z}{\tau_p} - 1}{\eta P_s xy}, (27d), \eta P_s xy \le \frac{P_s z}{\tau_p} - 1, (27e). \quad (27)$$

Based on Appendix A-1, the asymptotic behavior of J_1 can be determined.

On the other hand, J_2 can be reformulated as (28), given at the top of the next page.

Then, it follows from [30, Eq. (3.324.1)] that

$$J_2 \simeq \underbrace{\int_{\frac{\tau_p(\tau_0+1)}{P_s}}^{\infty} f_Z(z) \log_2\left(\frac{P_s z}{\tau_p}\right) J_{211}^{\infty} dz}_{\phi_1} - \underbrace{\int_{\frac{\tau_p(\tau_0+1)}{P_s}}^{\infty} f_Z(z) \log_2\left(\frac{P_s z}{\tau_p}\right) J_{212} dz}_{\phi_2}. \quad (29)$$

Utilizing the change of variables $u = \frac{P_s z}{\tau_p} - 1$ and $v = \frac{u}{P_s}$, we rewrite ϕ_1 as

$$\phi_1 \simeq \frac{\tau_p}{\lambda_{12}\lambda_{1B}\ln(2)} \sqrt{\frac{4\lambda_{1B}}{\lambda_{2B}\eta}} \left[\varpi_3 \ln(P_s) + \varpi_4\right], \quad (30)$$

where ϖ_3 and ϖ_4 are defined as $\varpi_3 \triangleq \lim_{P_s\to\infty} \int_{\frac{\tau_0}{P_s}}^{\infty} e^{-\frac{\tau_p v}{\lambda_{12}}} \sqrt{v} K_1\left(\sqrt{\frac{4v}{\lambda_{1B}\lambda_{2B}\eta}}\right) dv$ and $\varpi_4 \triangleq \lim_{P_s\to\infty} \int_{\frac{\tau_0}{P_s}}^{\infty} e^{-\frac{\tau_p v}{\lambda_{12}}} \ln(v) \sqrt{v} K_1\left(\sqrt{\frac{4v}{\lambda_{1B}\lambda_{2B}\eta}}\right) dv$. For ϕ_2, with the aid of the change of variables $u = \frac{P_s z}{\tau_p} - 1$ and $t = \frac{u}{\sqrt{P_s}}$, it follows from [30, Eqs. (3.381.3), (8.359.1), and (8.214.1)] that

$$\phi_2 \simeq \frac{1}{\ln(2)} \frac{\tau_p}{\lambda_{12}\lambda_{1B}P_s} \left[\frac{1}{4}\tau_0\lambda_{2B}(\ln(P_s))^2 + \frac{1}{2}\tau_0\lambda_{2B}\ln(P_s) \times \left(-C_{\text{Euler}} - \ln\left(\frac{\tau_0}{\lambda_{2B}}\right) + \frac{1}{2}\ln(\tau_0\eta) + \text{Ei}\left(-\frac{1}{\lambda_{2B}\sqrt{\tau_0\eta}}\right)\right) + \frac{1}{2}\tau_0^{\frac{3}{2}}\eta^{-\frac{1}{2}} \frac{\ln(P_s)}{\sqrt{P_s}} + \tau_0\lambda_{2B}\varpi_5\right], \quad (31)$$

which scales as $\frac{(\ln(P_s))^2}{P_s}$. Herein, we have $\varpi_5 \triangleq \lim_{P_s\to\infty} \int_{\frac{\tau_0}{\sqrt{P_s}}}^{1} t^{-1}\ln(t) e^{-\frac{t}{\lambda_{2B}}\sqrt{\frac{1}{\eta\tau_0}}} dt$. Summarizing the foregoing results, we establish the following proposition.

Proposition 4: When both T1 and T2 are required to decode $c(n)$ (Case I), the asymptotic behavior of the ergodic capacity of the backscatter link BD-T2 can be expressed as

$$C_{BC,T_{2,c}} \simeq \psi_0 \ln(P_s) + \psi_1, \quad (32)$$

in which $\psi_0 \triangleq \frac{1}{\ln(2)} + \frac{\sqrt{\frac{4\lambda_{1B}}{\lambda_{2B}\eta}}\left(\tau_p\varpi_3 - \frac{\varpi_1}{\sqrt{\tau_p}}\right)}{\lambda_{12}\lambda_{1B}\ln(2)}$ and $\psi_1 \triangleq \frac{\ln(\eta\lambda_{1B}\lambda_{2B}) - 2C_{\text{Euler}}}{\ln(2)} + \frac{\sqrt{\frac{4\lambda_{1B}}{\lambda_{2B}\eta}}}{\lambda_{12}\lambda_{1B}\ln(2)}\left[\tau_p\varpi_4 + \frac{\varpi_1\ln(\tau_p) - \varpi_0}{\sqrt{\tau_p}}\right] - \frac{\sqrt{\eta\tau_p\lambda_{12}\lambda_{1B}\lambda_{2B}}}{\lambda_{12}\ln(2)} e^{\frac{\lambda_{12}}{2\eta\tau_p\lambda_{1B}\lambda_{2B}}} W_{-0.5,0}\left(\frac{\lambda_{12}}{\eta\tau_p\lambda_{1B}\lambda_{2B}}\right)$, where $W_{a,b}(-)$ denotes the Whittaker W function and, ϖ_0, ϖ_1, ϖ_3, and ϖ_4 are defined as before.

Remark 4: It follows from Proposition 4 that the ergodic capacity scales linearly with respect to $\ln(P_s)$ in the high SNR regime, and the scaling coefficient is ψ_0. On the other hand, interestingly, as $P_s \to \infty$, it can be checked that $\tau_p\varpi_3 - \frac{\varpi_1}{\sqrt{\tau_p}} \to 0$ such that the scaling coefficient ψ_0 will not be affected by the channel statistics λ_{12}, λ_{1B}, and λ_{2B} for sufficiently high SNR. Note that at high SNR, the scaling rate of the ergodic capacity of the backscatter link BD-T2 in Case I is the same with the counterparts of the backscatter-NOMA and symbiotic radio systems in [22, Sect.IV.C]. Similar phenomenon can also be observed in Cases II and III, as will be shown by Propositions 5 and 6.

Now we turn to the ergodic capacity of the backscatter link BD-T1, which can be given by $C_{BC,T_{1,c}} = E\left[\log_2\left(1 + \gamma_{T_1,c}|_{\alpha=\alpha^*}\right)\right]$, where the expectation is taken over (8). Thus, we have

$$C_{BC,T_{1,c}} = E_{(8)}\left[\log_2\left(1 + \min\left[\eta P_s X^2, \frac{X\left(\frac{P_s Z}{\tau_p} - 1\right)}{Y}\right]\right)\right] = \underbrace{E_{(8),\ \eta P_s X \le \frac{1}{Y}\left(\frac{P_s Z}{\tau_p} - 1\right)}\left\{\log_2\left(1 + \eta P_s X^2\right)\right\}}_{S_1} + \underbrace{E_{(8),\ \eta P_s X > \frac{1}{Y}\left(\frac{P_s Z}{\tau_p} - 1\right)}\left\{\log_2\left(1 + \frac{X}{Y}\left(\frac{P_s Z}{\tau_p} - 1\right)\right)\right\}}_{S_2}. \quad (33)$$

By exchanging the integration order, we have

$$S_1 \simeq \frac{1}{\lambda_{1B}} e^{-\frac{\tau_p(\tau_0+1)}{\lambda_{12}P_s}} \log_2(\eta P_s) \underbrace{\int_{\sqrt{\frac{\tau_0}{\eta P_s}}}^{\infty} e^{-\frac{x}{\lambda_{1B}} - \frac{\tau_0}{\lambda_{2B}\eta P_s x}} dx}_{S_{11}} + \frac{2}{\lambda_{1B}} e^{-\frac{\tau_p(\tau_0+1)}{\lambda_{12}P_s}} \underbrace{\int_{\sqrt{\frac{\tau_0}{\eta P_s}}}^{\infty} e^{-\frac{x}{\lambda_{1B}} - \frac{\tau_0}{\lambda_{2B}\eta P_s x}} \log_2(x)\, dx}_{S_{12}} - \frac{1}{\lambda_{12}\lambda_{1B}} e^{-\frac{\tau_p(\tau_0+1)}{\lambda_{12}P_s}} \log_2(\eta P_s) \underbrace{\int_{\sqrt{\frac{\tau_0}{\eta P_s}}}^{\infty} \frac{e^{-\frac{x}{\lambda_{1B}} - \frac{\tau_0}{\lambda_{2B}\eta P_s x}}}{\frac{1}{\lambda_{12}} + \frac{1}{\tau_p\lambda_{2B}\eta x}} dx}_{S_{13}} - \frac{2}{\lambda_{12}\lambda_{1B}} e^{-\frac{\tau_p(\tau_0+1)}{\lambda_{12}P_s}} \underbrace{\int_{\sqrt{\frac{\tau_0}{\eta P_s}}}^{\infty} \frac{\log_2(x)\, e^{-\frac{x}{\lambda_{1B}} - \frac{\tau_0}{\lambda_{2B}\eta P_s x}}}{\frac{1}{\lambda_{12}} + \frac{1}{\tau_p\lambda_{2B}\eta x}} dx}_{S_{14}}. \quad (34)$$

By invoking Taylors series expansion of $e^{-\frac{\tau_0}{\lambda_{2B}\eta P_s x}}$ and with the aid of [30, Eq. (3.351.5)], we can arrive at $S_{11} \simeq \lambda_{1B} e^{-\frac{1}{\lambda_{1B}}\sqrt{\frac{\tau_0}{\eta P_s}}} + \frac{\tau_0}{\lambda_{2B}\eta P_s}\text{Ei}\left(-\frac{1}{\lambda_{1B}}\sqrt{\frac{\tau_0}{\eta P_s}}\right) \triangleq S_{11}^{\infty}$. Then, by utilizing [30, Eq. (8.212.1)] and after some algebraic manipulations, we have $S_{11} \simeq \lambda_{1B}$. By following a similar

$$J_2 = \int_{\frac{\tau_p(\tau_0+1)}{P_s}}^{\infty} f_Z(z) \log_2\left(\frac{P_s z}{\tau_p}\right) \underbrace{\iint_{x\geq\sqrt{\frac{\tau_0}{\eta P_s}}, y\leq\frac{1}{\tau_0}\left(\frac{P_s z}{\tau_p}-1\right)x, y>\frac{\frac{P_s z}{\tau_p}-1}{\eta P_s x}} f_X(x) f_Y(y) dx dy}_{J_{21}} dz. \tag{28}$$

procedure, S_{12} can be first asymptotically written as

$$S_{12} \simeq \frac{1}{\ln(2)} \int_{\sqrt{\frac{\tau_0}{\eta P_s}}}^{\infty} \ln(x) e^{-\frac{x}{\lambda_{1B}}} dx - \frac{\tau_0}{\lambda_{2B}\eta P_s \ln(2)} \underbrace{\int_{\sqrt{\frac{\tau_0}{\eta P_s}}}^{\infty} \frac{\ln(x)}{x} e^{-\frac{x}{\lambda_{1B}}} dx}_{\varpi_6}. \tag{35}$$

To proceed, we establish the following lemma regarding integrals of logarithm, exponential, and algebraic functions.

Lemma 2: For sufficiently high SNR, we have

$$\varpi_6 \triangleq \int_{\sqrt{\frac{\tau_0}{\eta P_s}}}^{\infty} \frac{\ln(x)}{x} e^{-\frac{x}{\lambda_{1B}}} dx \propto [\log(P_s)]^2,$$
$$\varpi_7 \triangleq \int_{\sqrt{\frac{\tau_0}{\eta P_s}}}^{\infty} \frac{\ln(x) e^{-\frac{x}{\lambda_{1B}}}}{x + \frac{\lambda_{12}}{\tau_p \lambda_{2B} \eta}} dx \to \text{Constant}. \tag{36}$$

Proof: By utilizing L'Hôpital's rule and after some algebraic manipulations, we complete the proof of Lemma 2. □

Now, by using [30, Eqs. (4.352.1) and (8.366.1)] and knowing that $\varpi_6 \propto [\log(P_s)]^2$, we can attain $S_{12} \simeq \frac{\lambda_{1B}}{\ln(2)}\left[-C_{\text{Euler}} + \ln(\lambda_{1B})\right] \triangleq S_{12}^{\infty}$. Next, with the aid of [30, Eq. (3.352.2)] and after several arrangements, we have $S_{13} \simeq \lambda_{12}\lambda_{1B} + \frac{\lambda_{12}^2}{\eta\tau_p\lambda_{2B}} e^{\frac{\lambda_{12}}{\eta\tau_p\lambda_{1B}\lambda_{2B}}} \text{Ei}\left(-\frac{\lambda_{12}}{\eta\tau_p\lambda_{1B}\lambda_{2B}}\right) \triangleq S_{13}^{\infty}$. Using [30, Eq. (4.331.2)], we have

$$S_{14} \simeq \frac{\lambda_{12}}{\ln(2)}\left[-\lambda_{1B}\left(C_{Euler} + \ln\left(\frac{1}{\lambda_{1B}}\sqrt{\frac{\tau_0}{\eta P_s}}\right)\right) + \lambda_{1B}\ln\left(\sqrt{\frac{\tau_0}{\eta P_s}}\right) e^{-\frac{1}{\lambda_{1B}}\sqrt{\frac{\tau_0}{\eta P_s}}}\right] - \frac{\lambda_{12}^2 \varpi_7}{\eta\tau_p\lambda_{2B}\ln(2)} \triangleq S_{14}^{\infty}, \tag{37}$$

where ϖ_7 approaches to a constant in the high SNR regime. By substituting the above results into S_1, the scaling behavior of S_1 can be characterized.

Turning our attentions to S_2, it follows from Appendix A-2 that an asymptotic expression of S_2 can be written as (38), shown at the top of the following page. To summarize, we can arrive at the following proposition.

Proposition 5: When both T1 and T2 are required to decode $c(n)$ (Case I), the ergodic capacity of the backscatter link BD-T1 can be asymptotically written as

$$C_{BC,T_{1,c}} \simeq \frac{\ln(P_s)}{\ln(2)} + \frac{1}{\ln(2)}\left[\ln\left(\frac{\lambda_{1B}}{\lambda_{2B}}\right) + \frac{\lambda_{12}}{\eta\tau_p\lambda_{1B}\lambda_{2B}}\varpi_7 - C_{Euler} - \frac{\lambda_{12}}{\lambda_{1B}}\varpi_8\right] - \frac{\lambda_{12}\ln(\eta\lambda_{2B})}{\eta\tau_p\lambda_{1B}\lambda_{2B}\ln(2)} e^{\frac{\lambda_{12}}{\eta\tau_p\lambda_{1B}\lambda_{2B}}} \text{Ei}\left(-\frac{\lambda_{12}}{\eta\tau_p\lambda_{1B}\lambda_{2B}}\right) - \underbrace{\frac{\tau_p}{\lambda_{12}\ln(2)} \int_{\sqrt{\frac{\tau_0}{\eta P_s}}}^{\infty} f_X(x) \frac{\ln\left(\frac{\tau_p}{\lambda_{12}} + \frac{1}{\lambda_{2B}\eta x}\right)}{\frac{\tau_p}{\lambda_{12}} + \frac{1}{\lambda_{2B}\eta x}} dx}_{\wp}. \tag{39}$$

B. Only T2 Decodes $c(n)$

In this case, to boost the rate of the backscatter link from BD to T2, the reflection coefficient α is set to $\alpha = \hat{\alpha} \triangleq \min\left[1, \frac{\frac{P_s|h_{12}|^2}{\tau_p}-1}{\eta P_s |h_{1B}|^2 |h_{2B}|^2}\right]$ such that $C_{BC,T_2} = E\left\{\log_2\left(1+\gamma_{T_2,c}\big|_{\alpha=\hat{\alpha}}\right)\right\}$, where the expectation operator is taken under the following conditions:

$$\frac{\tau_0}{\eta P_s |h_{1B}|^2 |h_{2B}|^2} \leq 1, \tau_0 \leq \frac{P_s |h_{12}|^2}{\tau_p} - 1. \tag{40}$$

By its turn, we have

$$C_{BC,T_2} = \underbrace{E_{\substack{(40),\\ \eta P_s XY \leq \frac{P_s Z}{\tau_p}-1}} \{\log_2(1+\eta P_s XY)\}}_{\text{K}_1} + \underbrace{E_{\substack{(40),\\ \eta P_s XY > \frac{P_s Z}{\tau_p}-1}} \left\{\log_2\left(\frac{P_s Z}{\tau_p}\right)\right\}}_{\text{K}_2}. \tag{41}$$

As $P_s \to \infty$, K_1 can be asymptotically written as

$$\text{K}_1 \simeq \underbrace{E_{\substack{(40),\\ \eta P_s XY \leq \frac{P_s Z}{\tau_p}-1}} \{\log_2(P_s)\}}_{\text{K}_{11}} + \underbrace{E_{\substack{(40),\\ \eta P_s XY \leq \frac{P_s Z}{\tau_p}-1}} \{\log_2(\eta XY)\}}_{\text{K}_{12}}, \tag{42}$$

where K_{11} can be calculated as $\text{K}_{11} \simeq \log_2(P_s)\text{K}_{111}^{\infty} \triangleq \log_2(P_s)\left(1 - \sqrt{\frac{4}{\lambda_{1B}\lambda_{2B}\eta}}\frac{\tau_p}{\lambda_{12}}\varpi_3\right)$, by invoking [30, Eq. (3.471.9)] and the change of variables $u = \frac{P_s z}{\tau_p} - 1$ and $v = \frac{u}{P_s}$. On the other hand, K_{12} can be re-expressed as

$$\text{K}_{12} = \int_{\frac{\tau_p(\tau_0+1)}{P_s}}^{\infty} f_Z(z) \int_0^{\infty} f_X(x) \underbrace{\int_{\frac{\tau_0}{\eta P_s x}}^{\frac{\frac{P_s z}{\tau_p}-1}{\eta P_s x}} f_Y(y) \log_2(\eta x y) dy}_{\epsilon_0} dx dz. \tag{43}$$

In what follows, we characterize the high-SNR behavior of K_{12}.

Lemma 3: For sufficiently high SNR, K_{12} can be asymptotically written as

$$\text{K}_{12} \simeq \frac{-2C_{\text{Euler}} + \ln(\eta\lambda_{1B}\lambda_{2B})}{\ln(2)} - \frac{2}{\lambda_{12}\ln(2)\sqrt{\eta\tau_p\lambda_{1B}\lambda_{2B}}}\left[\varpi_0 - \ln(\tau_p)\varpi_1\right] - \frac{\sqrt{\eta\tau_p\lambda_{12}\lambda_{1B}\lambda_{2B}}}{\lambda_{12}\ln(2)} e^{\frac{\lambda_{12}}{2\eta\tau_p\lambda_{1B}\lambda_{2B}}} W_{-0.5,0}\left(\frac{\lambda_{12}}{\eta\tau_p\lambda_{1B}\lambda_{2B}}\right). \tag{44}$$

$$S_2 \simeq \ln\left(P_s\right)\left[\frac{1}{\ln\left(2\right)}+\frac{\lambda_{12}}{\eta\tau_p\lambda_{1B}\lambda_{2B}\ln\left(2\right)}e^{\frac{\lambda_{12}}{\eta\tau_p\lambda_{1B}\lambda_{2B}}}\mathrm{Ei}\left(-\frac{\lambda_{12}}{\eta\tau_p\lambda_{1B}\lambda_{2B}}\right)\right]+\frac{1}{\ln\left(2\right)}\left[\ln\left(\frac{\lambda_{1B}}{\lambda_{2B}}\right)-\frac{\lambda_{12}}{\eta\tau_p\lambda_{1B}\lambda_{2B}}\varpi_7-C_{Euler}-\frac{\lambda_{12}}{\lambda_{1B}}\varpi_8\right]$$
$$-\frac{\lambda_{12}\ln\left(\lambda_{2B}\right)}{\eta\tau_p\lambda_{1B}\lambda_{2B}\ln\left(2\right)}e^{\frac{\lambda_{12}}{\eta\tau_p\lambda_{1B}\lambda_{2B}}}\mathrm{Ei}\left(-\frac{\lambda_{12}}{\eta\tau_p\lambda_{1B}\lambda_{2B}}\right)-\frac{\tau_p}{\lambda_{12}\ln\left(2\right)}\int_{\sqrt{\frac{\tau_0}{\eta P_s}}}^{\infty}f_X\left(x\right)\frac{\ln\left(\frac{\tau_p}{\lambda_{12}}+\frac{1}{\lambda_{2B}\eta x}\right)}{\frac{\tau_p}{\lambda_{12}}+\frac{1}{\lambda_{2B}\eta x}}dx. \quad (38)$$

Proof: Please refer to Appendix A-3. □

Summarizing the foregoing results, an asymptotic expression can be derived for K_1. For K_2, by using [30, Eq. (3.471.9)], the change of variables $u=\frac{P_s z}{\tau_p}-1$, $v=\frac{u}{P_s}$, and after several algebraic manipulations, it follows from (41) that

$$\begin{aligned}\mathrm{K}_2 &\simeq \sqrt{\frac{4}{\eta\lambda_{1B}\lambda_{2B}}}\frac{\tau_p}{\lambda_{12}}\\ &\times\lim_{P_s\to\infty}\int_{\frac{\tau_0}{P_s}}^{\infty}e^{-\frac{\tau_p v}{\lambda_{12}}}\left[\log_2\left(P_s v\right)\right]\sqrt{v}K_1\left(\sqrt{\frac{4v}{\eta\lambda_{1B}\lambda_{2B}}}\right)dv\\ &=\frac{\tau_p}{\lambda_{12}\ln\left(2\right)}\sqrt{\frac{4}{\eta\lambda_{1B}\lambda_{2B}}}\left[\ln\left(P_s\right)\varpi_3+\varpi_4\right], \quad (45)\end{aligned}$$

where ϖ_3 and ϖ_4 are the same as before. It is noteworthy that (45) is exactly the same with (30). Summarizing the foregoing results, one can establish the following proposition.

Proposition 6: At high SNR, when only T2 decodes $c(n)$ (Case II), the ergodic capacity of the backscatter link BD-T2 is exactly the same with (32).

Remark 5: One can observe that at high SNR, the ergodic capacity of the backscatter link BD-T2 remains unchanged regardless of whether the terminal T1 is required to decode $c(n)$. In other words, the effects of decoding operation at T1 to decode $c(n)$ on the ergodic capacity of the backscatter link BD-T2 disappears in the high SNR regions.

C. Only T1 Decodes $c(n)$

In this case, we evaluate the ergodic capacity of the backscatter link BD-T1. To guarantee that T1 can successfully decode $c(n)$ while T2 can successfully decode $s(n)$, the reflection coefficient α has to satisfy $\frac{\tau_0}{\eta P_s|h_{1B}|^4}\leq\alpha\leq\frac{\frac{P_s|h_{12}|^2}{\tau_p}-1}{\eta P_s|h_{1B}|^2|h_{2B}|^2}$. To boost the rate of the backscatter link, α is set to $\alpha=\breve{\alpha}=\min\left[1,\frac{\frac{P_s|h_{12}|^2}{\tau_p}-1}{\eta P_s|h_{1B}|^2|h_{2B}|^2}\right]$. Accordingly, the ergodic capacity can be written as $C_{BC,T_1}=E\left\{\log_2\left(1+\gamma_{T_1,c}|_{\alpha=\breve{\alpha}}\right)\right\}$, where the expectation is taken over the following domain:

$$\frac{\tau_0}{\eta P_s\left|h_{1B}\right|^4}\leq 1,\frac{\tau_0}{\left|h_{1B}\right|^2}\leq\frac{\frac{P_s|h_{12}|^2}{\tau_p}-1}{\left|h_{2B}\right|^2},\frac{P_s\left|h_{12}\right|^2}{\tau_p}-1\geq 0. \quad (46)$$

Furthermore, the ergodic capacity can be expressed as

$$\begin{aligned}C_{BC,T_1}=&\underbrace{E_{(46),\ \eta P_s X^2\leq\frac{X}{Y}\left(\frac{P_s Z}{\tau_p}-1\right)}\left\{\log_2\left(1+\eta P_s X^2\right)\right\}}_{L_1}\\ &+\underbrace{E_{(46),\ \eta P_s X^2>\frac{X}{Y}\left(\frac{P_s Z}{\tau_p}-1\right)}\left\{\log_2\left(1+\frac{X}{Y}\left(\frac{P_s Z}{\tau_p}-1\right)\right)\right\}}_{L_2}. \quad (47)\end{aligned}$$

By exchanging the integration order and invoking [30, Eqs. (3.352.2) and (4.331.2)], we have

$$\begin{aligned}L_1 &\simeq -\frac{\lambda_{12}}{\lambda_{1B}\lambda_{2B}\eta\tau_p\ln\left(2\right)}\\ &\times\left[\left(\ln\left(\eta\right)+\ln\left(P_s\right)\right)e^{\frac{\lambda_{12}}{\lambda_{1B}\lambda_{2B}\eta\tau_p}}\mathrm{Ei}\left(-\frac{\lambda_{12}}{\lambda_{1B}\lambda_{2B}\eta\tau_p}\right)-2\varpi_7\right]\\ &\propto\log\left(P_s\right). \quad (48)\end{aligned}$$

Next, we focus on L_2. According to Appendix A-4, an asymptotic expression of L_2 can be achieved. Therefore, one can attain an asymptotic expression of $C_{BC,T_1}\propto\log\left(P_s\right)$, which is summarized as follows.

Proposition 7: In the high SNR regions, when only T1 decodes $c(n)$ (Case III), the ergodic capacity of the backscatter link BD-T1 can be asymptotically written as

$$\begin{aligned}C_{BC,T_1}\simeq&\frac{\ln\left(P_s\right)}{\ln\left(2\right)}+\frac{2\left(\ln\left(\lambda_{1B}\right)-C_{Euler}\right)+\ln\left(\eta\right)}{\ln\left(2\right)}\\ &-\frac{e^{\frac{\lambda_{12}}{2\eta\tau_p\lambda_{1B}\lambda_{2B}}}}{\ln\left(2\right)}\sqrt{\frac{\eta\tau_p\lambda_{1B}\lambda_{2B}}{\lambda_{12}}}W_{-0.5,0}\left(\frac{\lambda_{12}}{\eta\tau_p\lambda_{1B}\lambda_{2B}}\right). \quad (49)\end{aligned}$$

We are curious to know the capacity difference between (49) and (39), in order to understand the effects of decoding operation of $c(n)$ at T2 on the backscatter reception at T1, which is given as below.

Proposition 8: For sufficiently high SNR, the ergodic capacity of the backscatter link BD-T1 is not affected by the decoding operation of $c(n)$ at T2.

Proof: Please refer to Appendix A-9.

Remark 6: For the metric of ergodic capacity, it follows from Propositions 6 and 8 that the impacts of decoding operation of $c(n)$ at T1 or T2 gradually disappears at high SNR, which is different from the impacts of these decoding constraints on the coexistence outage probability as shown in Propositions 1-3. This means that the impacts of decoding constraints on the different performance metrics are dramatically different.

V. Numerical Results and Discussion

In this section, we first validate the analytical results presented in the foregoing sections, and then examine the observations made from the theoretical analysis via Monte-Carlo simulations.

A. Outage Behavior

Fig. 3 shows the coexistence outage probability where primary and backscatter transmissions coexist. It is first observed that the asymptotic outage curves match well with simulations at least in the medium and high SNR regions. Also, it can be seen that the outage curve for the scenario where both T1 and T2 decode $c(n)$ approaches toward that of the scenario where only T1 decodes $c(n)$, as predicted in the foregoing remarks. This is because the restriction condition of decoding $c(n)$ at T1 results in a dominating term $\frac{1}{\sqrt{P_s}}$ for the coexistence outage

This article has been accepted for publication in IEEE Internet of Things Journal. This is the author's version which has not been fully edited and content may change prior to final publication. Citation information: DOI 10.1109/JIOT.2022.3188570

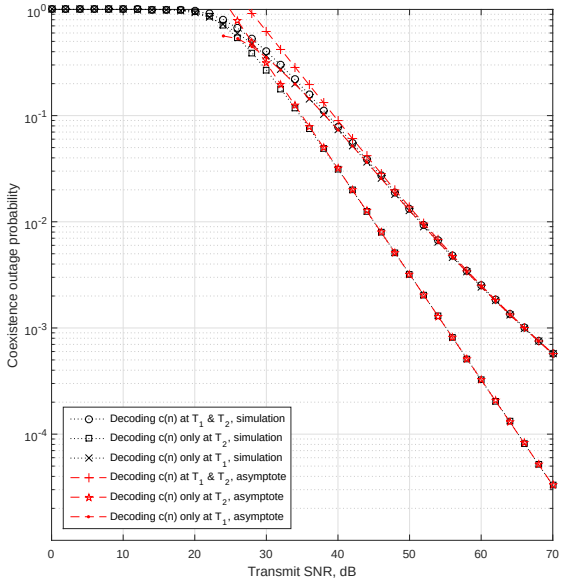

Fig. 3: Coexistence outage probability of the symbiotic AmBC systems.

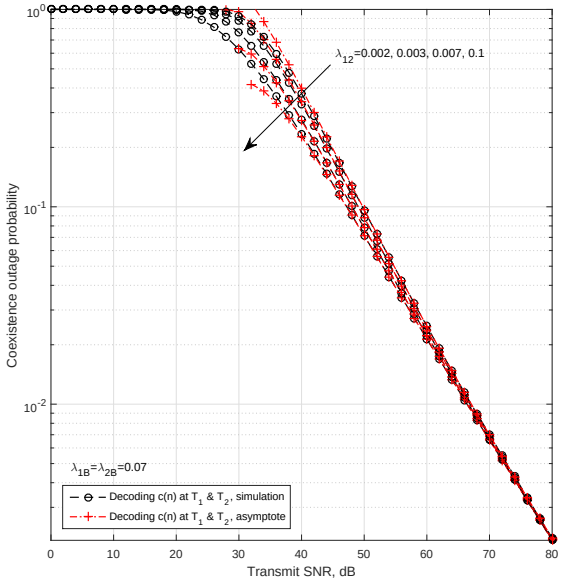

Fig. 5: Coexistence outage probability when both T1 and T2 decode $c(n)$.

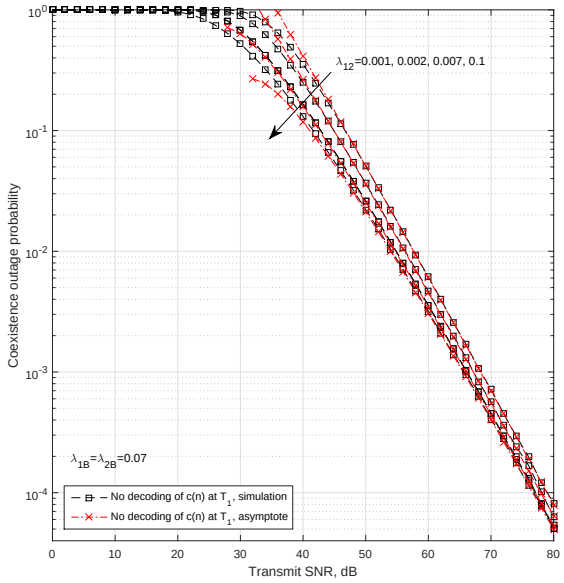

Fig. 4: Coexistence outage probability when only T2 decodes $c(n)$.

probability at high SNR, whereas the impacts of the restriction condition of decoding $c(n)$ at T2 on the coexistence outage probability tend to be marginal relative to $\frac{1}{\sqrt{P_s}}$ at high SNR. For small values of transmit SNR, it follows from (8), (17), and (22) that the coexistence outage probability of Cases I, II, and III tends to the same limit, i.e., unity, as shown by Fig. 3.

Fig. 4 illustrates the coexistence outage probability when only T2 decodes $c(n)$ while T1 is not required to do so. It is shown that the outage performance improves dramatically with an increase in the average channel gain λ_{12} especially in the low and medium SNR regions, which is in accord with (21). However, in the high SNR regions, the outage curves with different values of λ_{12} tend to converge but always with a noticeable gap among them. This is due to the fact that in the asymptotic expression given by (21), the term with λ_{12} acts as a dominant ingredient in the high SNR regions. Note that this phenomenon is different from the scenario where T1 is required to decode $c(n)$. Unlike Fig. 4, it follows from Fig. 5 that when both T1 and T2 are required to decode $c(n)$, the coexistence outage probability converges in the high SNR regions regardless of the value of λ_{12}, which is in accord with (16). As shown in Fig. 6, when only T1 is required to decode $c(n)$, the high-SNR outage behavior is again not affected by the average channel gain λ_{12}, as in the scenario where both T1 and T2 are required to decode $c(n)$. This accords with (23). On the other hand, the coexistence outage performance improves with an increase in the average channel gain λ_{1B}, as predicted by (23).

B. Ergodic Capacity

Fig. 7 shows the ergodic capacity of the backscatter links when both T1 and T2 decode $c(n)$. It can be first seen that the asymptotic curves match well with simulations in the medium and high SNR regions, which confirms our theoretical analysis. In addition, it is shown that the ergodic capacity of the backscatter link T1-BD-T2 is always larger than that of the backscatter link T1-BD-T1 and the capacity gap gradually narrows with the improvement of the channel conditions. This means that under good channel conditions, the ergodic capacity of the two backscatter links turns out to be comparable to each other.

Fig. 8 demonstrates the ergodic capacity of the backscatter link when only T1 or T2 decodes $c(n)$. Once again, the accuracy of our asymptotic analytical results is first confirmed. As in the scenario where both T1 and T2 decode $c(n)$, the ergodic capacity of the backscatter link when only T2 decodes $c(n)$ outperforms the counterpart when only T1 decodes $c(n)$, and the performance gap shrinks as the channel conditions become better as before.

This article has been accepted for publication in IEEE Internet of Things Journal. This is the author's version which has not been fully edited and content may change prior to final publication. Citation information: DOI 10.1109/JIOT.2022.3188570

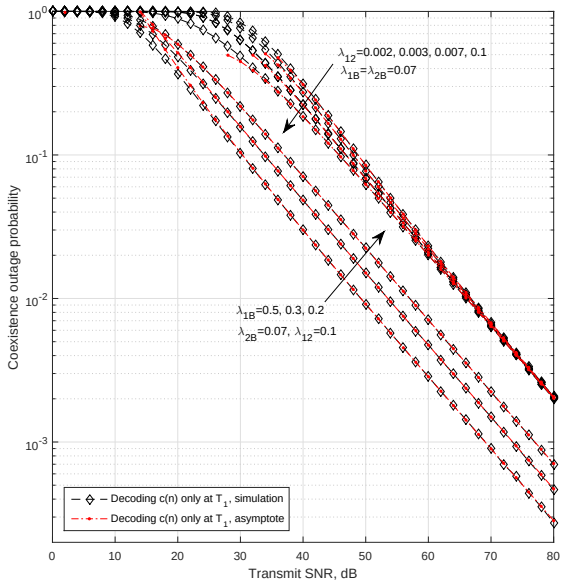

Fig. 6: Coexistence outage probability when only T1 decodes $c(n)$.

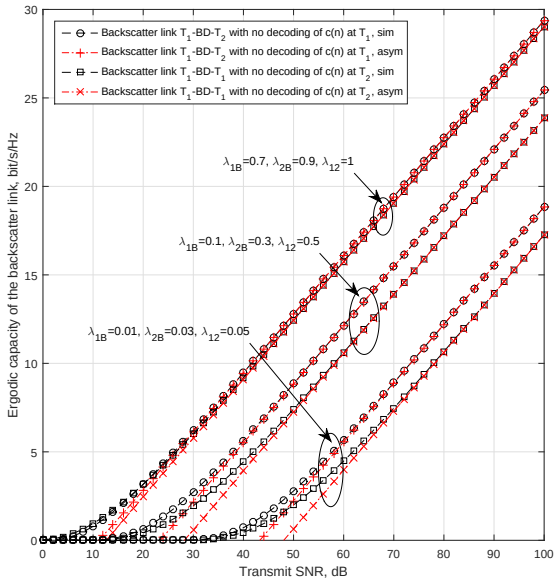

Fig. 8: Ergodic capacity of the backscatter link when only T1 or T2 decodes $c(n)$.

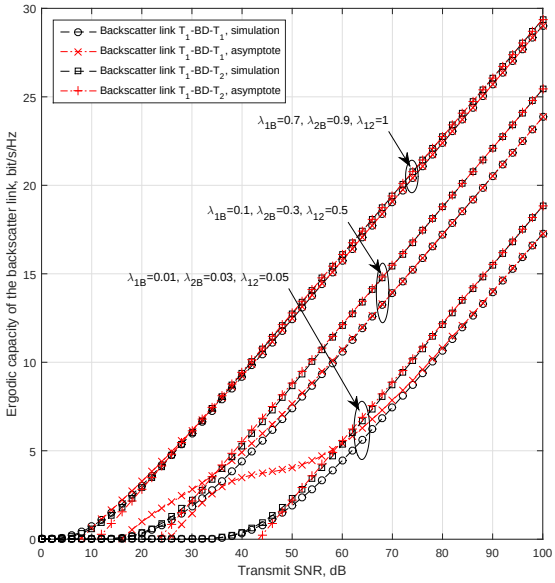

Fig. 7: Ergodic capacity of the backscatter link when both T1 and T2 decode $c(n)$.

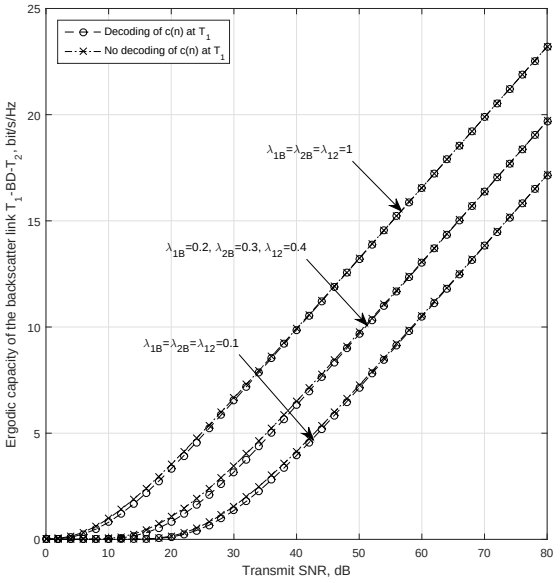

Fig. 9: On the effects of decoding of $c(n)$ on the ergodic capacity of the backscatter link BD-T2.

In what follows, we try to discover the effects of decoding operation of $c(n)$ on the ergodic capacity of the backscatter links. Fig. 9 makes a comparison of the ergodic capacity of the backscatter link BD-T2 between the case of decoding $c(n)$ at T1 and the case of no decoding of $c(n)$ at T1. As shown by the figure, when the decoding requirement of $c(n)$ is removed at T1, the ergodic capacity of the backscatter link T1-BD-T2 increases, especially in the low and medium SNR regions. Nonetheless, in the high SNR regions, the capacity improvement owing to the removal of decoding operation of $c(n)$ at T1 gradually disappears, which complies with Remark 5. In another word, the effects of decoding operation of $c(n)$ at T1 on the ergodic capacity of the backscatter link BD-T2 becomes barely noticeable in the high SNR regions. Similarly, it can be observed from Fig. 10 that the removal of decoding operation of $c(n)$ at T2 can indeed boost the ergodic capacity of the backscatter link T1-BD-T1 at least in the low and medium SNR regions. However, this performance improvement lessens with an increase in transmit SNR and finally disappears at high SNR, which is predicted by Proposition 8.

To make a pertinent comparison with [22], Figure 11 considers the scenario of Case II where no decoding operation

This article has been accepted for publication in IEEE Internet of Things Journal. This is the author's version which has not been fully edited and content may change prior to final publication. Citation information: DOI 10.1109/JIOT.2022.3188570

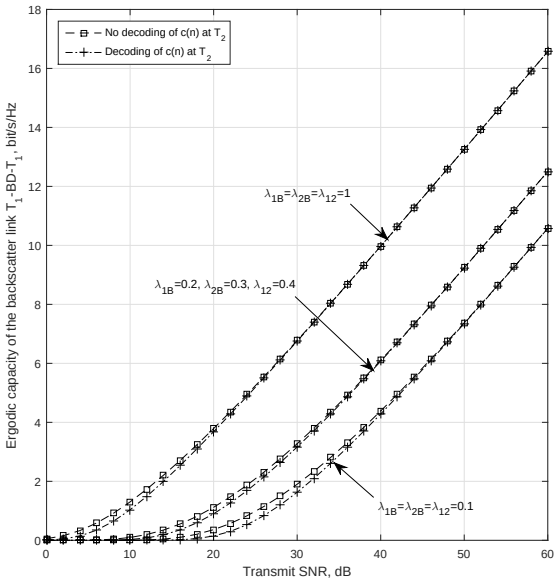

Fig. 10: On the effects of decoding of $c(n)$ on the ergodic capacity of the backscatter link BD-T1.

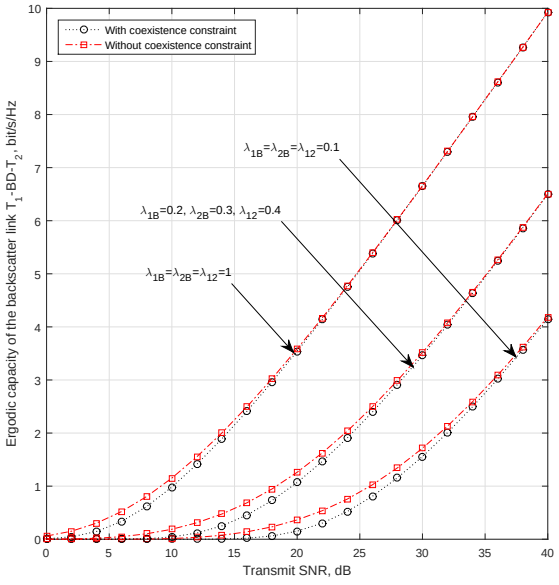

Fig. 11: Effects of coexistence constraint on the ergodic capacity of the backscatter channel in Case II.

of $c(n)$ is required at T1. It is shown that when the coexistence constraint (i.e., Eq. (40) in this case) was removed to calculate the ergodic capacity, the capacity performance naturally improves, which complies with the definition of ergodic capacity. Also, with the improvement of channel conditions, the performance gap between the curve with coexistence constraint and that without coexistence constraint narrows. Nonetheless, the removing of such a coexistence constraint may lead to an information transmission outage of the backscatter link according to Section III. For the metric of coexistence outage probability, similar phenomenon can be observed, which is omitted here due to space limit.

C. Advantages of Different Scenarios

Based on the forgoing results, it is ready to confirm that for Case I, the advantage is that both T1 and T2 could attain the information $c(n)$ at BD, whereas the disadvantage is that the CSI of the loop-interference channel has to be attained at T1 to cancel its self-interference signal $s(n)$ such that $c(n)$ can be decoded at T1. Relative to Case I, the advantage of Case II is that the COP of the symbiotic AmBC system can be improved by removing the constraint of decoding operation of $c(n)$ at T1. Also, by removing the decoding operation of $c(n)$ at T1, the round-trip fading effects of the BD-T1 channel to decode $c(n)$ are eliminated, resulting in a steeper decreasing rate of the COP (i.e., a scaling law of $\frac{\ln(P_s)}{P_s}$). In comparing with Case I, the COP of Case III can also be improved by removing the decoding operation of $c(n)$ at T2 but the COP still suffers from the round-trip fading effects of the $BD \to T1$ channel (i.e., a scaling law of $\frac{1}{\sqrt{P_s}}$). In addition, in comparison with Case I, both Cases II and III lead to a higher ergodic capacity of the backscatter channels as shown by Figures 9 and 10.

VI. Concluding Remarks

In this paper, we characterized the scaling behavior of coexistence outage probability and ergodic capacity for a symbiotic AmBC system, in which a source T1 communicates with a destination T2, whereas a backscatter device BD also passively conveys its own information $c(n)$ to T1 and/or T2 via backscattering links. Particularly, we considered three cases for the symbiotic AmBC system. It was shown that the restriction condition of decoding $c(n)$ at T1 leads to a dominating term $\frac{1}{\sqrt{P_s}}$ for the coexistence outage probability at high SNR, whereas the impacts of the restriction condition of decoding $c(n)$ at T2 on the coexistence outage probability tends to lessen at high SNR. Also, under different cases, the impacts of the channel statistics of the link T1-T2 on the coexistence outage probability were shown to be radically different. Finally, the ergodic capacity of the backscatter link was analyzed at high SNR for the three cases and their relationship was disclosed as well.

Appendix A

A-1: Asymptotic Behavior of J_1

Firstly, (26) can be expressed as (A.1), shown at the top of the next page. With the aid of [30, Eq. (4.331.2)] and the change of variables $u = 1 + \eta P_s xy$, J_{11} in (A.1) can be rewritten as (A.2), shown at the top of the next page. In what follows, we first concentrate on the analysis of $\hat{J}_1$. Utilizing [30, Eqs. (3.351.4) and (8.214.1)] and after some algebraic manipulations, $\hat{J}_1$ can be asymptotically written as

$$\hat{J}_1 \simeq \lambda_{1B}\left[1 - \frac{1}{\lambda_{1B}}\sqrt{\frac{\tau_0}{\eta P_s}} + \frac{1}{2}\left(\frac{1}{\lambda_{1B}}\right)^2 \frac{\tau_0}{\eta P_s}\right] + \frac{\tau_0}{\lambda_{2B}\eta P_s}\left[C_{\text{Euler}} + \ln\left(\frac{1}{\lambda_{1B}}\sqrt{\frac{\tau_0}{\eta P_s}}\right)\right] \triangleq \hat{J}_1^{\infty}. \quad \text{(A.3)}$$

Invoking the change of variables $t = \frac{x}{\sqrt{\frac{\tau_0}{\eta P_s}}}$ and utilizing [30, Eqs. (4.331.2) and (3.351.4)], $\hat{J}_2$ can be asymptotically written

$$J_1 = \int_{\frac{(\tau_0+1)\tau_p}{P_s}}^{\infty} f_Z(z) \underbrace{\iint_{(27a),(27c),(27d),(27e)} f_X(x) f_Y(y) \log_2(1+\eta P_s xy)\, dxdy}_{J_{11}} dz. \tag{A.1}$$

$$J_{11} = \frac{\ln(1+\tau_0)}{\lambda_{1B}\ln(2)} \underbrace{\int_{\sqrt{\frac{\tau_0}{\eta P_s}}}^{\infty} e^{-\frac{x}{\lambda_{1B}} - \frac{\tau_0}{\lambda_{2B}\eta P_s x}} dx}_{\hat{J}_1} - \frac{1}{\lambda_{1B}\ln(2)} \underbrace{\int_{\sqrt{\frac{\tau_0}{\eta P_s}}}^{\infty} e^{-\frac{x}{\lambda_{1B}} + \frac{1}{\lambda_{2B}\eta P_s x}} \mathrm{Ei}\left(-\frac{1+\tau_0}{\lambda_{2B}\eta P_s x}\right) dx}_{\hat{J}_2}$$
$$- \frac{\ln\left(\frac{zP_s}{\tau_p}\right)}{\lambda_{1B}\ln(2)} \underbrace{\int_{\sqrt{\frac{\tau_0}{\eta P_s}}}^{\infty} e^{-\frac{x}{\lambda_{1B}} - \frac{1}{x}\left(\frac{z}{\eta\tau_p\lambda_{2B}} - \frac{1}{\lambda_{2B}\eta P_s}\right)} dx}_{\hat{J}_3} + \frac{1}{\lambda_{1B}\ln(2)} \underbrace{\int_{\sqrt{\frac{\tau_0}{\eta P_s}}}^{\infty} e^{-\frac{x}{\lambda_{1B}} + \frac{1}{\lambda_{2B}\eta P_s x}} \mathrm{Ei}\left(-\frac{z}{\eta\tau_p\lambda_{2B}x}\right) dx}_{\hat{J}_4}. \tag{A.2}$$

as

$$\hat{J}_2 \simeq 2\lambda_{1B}C_{\text{Euler}} + \lambda_{1B}\ln\left(\frac{1+\tau_0}{\lambda_{2B}\eta P_s}\right) + \lambda_{1B}\ln\left(\frac{1}{\lambda_{1B}}\right) + \sqrt{\frac{\tau_0}{\eta P_s}}\left[-C_{\text{Euler}} - \ln\left(\frac{1+\tau_0}{\lambda_{2B}\eta P_s}\right) + \ln\left(\sqrt{\frac{\tau_0}{\eta P_s}}\right) - 1\right] \triangleq \hat{J}_2^{\infty}. \tag{A.4}$$

For $\hat{J}_3$ and $\hat{J}_4$, by invoking [30, Eq. (3.324.1)], they can be asymptotically written as

$$\hat{J}_3 \simeq \int_0^{\infty} e^{-\frac{x}{\lambda_{1B}} - \frac{z}{\eta\tau_p\lambda_{2B}x}} dx = \sqrt{\frac{4z\lambda_{1B}}{\eta\tau_p\lambda_{2B}}} K_1\left(\sqrt{\frac{4z}{\eta\tau_p\lambda_{1B}\lambda_{2B}}}\right) \triangleq \hat{J}_3^{\infty}. \tag{A.5}$$

$$\hat{J}_4 \simeq \int_0^{\infty} e^{-\frac{x}{\lambda_{1B}}} \mathrm{Ei}\left(-\frac{z}{\eta\tau_p\lambda_{2B}x}\right) dx = -2\lambda_{1B}K_0\left(\sqrt{\frac{4z}{\eta\tau_p\lambda_{1B}\lambda_{2B}}}\right) \triangleq \hat{J}_4^{\infty}. \tag{A.6}$$

where the last step is achieved by making use of the change of variables $u = \frac{\eta\tau_p\lambda_{2B}x}{4z}$ and invoking [30, Eq. (6.226.1)]. Next, by substituting $\hat{J}_1$, $\hat{J}_2$, $\hat{J}_3$, and $\hat{J}_4$ into (A.2), and then plugging the latter into (A.1), we can achieve an asymptotic expression for J_1. To proceed, we first substitute $\hat{J}_1^{\infty}$ into J_1 and attain

$$J_1\left(\hat{J}_1^{\infty}\right) \simeq \frac{\ln(1+\tau_0)}{\ln(2)}\left(1 - \frac{1}{\lambda_{1B}}\sqrt{\frac{\tau_0}{\eta P_s}}\right) \simeq \log_2(1+\tau_0). \tag{A.7}$$

In a similar way, we can achieve

$$J_1\left(\hat{J}_2^{\infty}\right) \simeq \frac{-1}{\lambda_{1B}\ln(2)}\left\{2\lambda_{1B}C_{\text{Euler}} + \lambda_{1B}\ln\left(\frac{1+\tau_0}{\lambda_{2B}\eta P_s}\right) + \lambda_{1B}\ln\left(\frac{1}{\lambda_{1B}}\right) + \sqrt{\frac{\tau_0}{\eta P_s}}\left(-C_{\text{Euler}} - \ln\left(\frac{1+\tau_0}{\lambda_{2B}\eta P_s}\right) + \ln\left(\sqrt{\frac{\tau_0}{\eta P_s}}\right) - 1\right)\right\}. \tag{A.8}$$

As can be observed by (A.8), as $P_s \to \infty$, the scaling law of $J_1\left(\hat{J}_2^{\infty}\right)$ is $\log(P_s)$. By its turn, we have

$$J_1\left(\hat{J}_3^{\infty}\right) \simeq -\frac{\sqrt{\frac{4\lambda_{1B}}{\eta\tau_p\lambda_{2B}}}}{\lambda_{12}\lambda_{1B}\ln(2)}\varpi_0 - \frac{\sqrt{\frac{4\lambda_{1B}}{\eta\tau_p\lambda_{2B}}}}{\lambda_{12}\lambda_{1B}\ln(2)}\ln\left(\frac{P_s}{\tau_p}\right)\varpi_1, \tag{A.9}$$

where ϖ_0 and ϖ_1 can be calculated as $\varpi_0 = \int_0^{\infty}\sqrt{z}\ln(z)\, e^{-\frac{z}{\lambda_{12}}} K_1\left(\sqrt{\frac{4z}{\eta\tau_p\lambda_{1B}\lambda_{2B}}}\right) dz$ and $\varpi_1 = \int_0^{\infty}\sqrt{z} e^{-\frac{z}{\lambda_{12}}} K_1\left(\sqrt{\frac{4z}{\eta\tau_p\lambda_{1B}\lambda_{2B}}}\right) dz$, respectively. Since both ϖ_0 and ϖ_1 are irrelevant constants with regard to P_s, it follows that $J_1\left(\hat{J}_3^{\infty}\right)$ also scales as $\log(P_s)$ in the high SNR regime. Finally, for $\hat{J}_4^{\infty}$, we have $J_1\left(\hat{J}_4^{\infty}\right) \simeq \frac{-2}{\lambda_{12}\ln(2)}\int_0^{\infty} e^{-\frac{z}{\lambda_{12}}} K_0\left(2\sqrt{\frac{z}{\eta\tau_p\lambda_{1B}\lambda_{2B}}}\right) dz \triangleq \varpi_2$. With the aid of [30, Eq. (6.614.4)], $J_1\left(\hat{J}_4^{\infty}\right)$ can be further asymptotically expressed as

$$J_1\left(\hat{J}_4^{\infty}\right) \simeq -\frac{\sqrt{\lambda_{12}\eta\tau_p\lambda_{1B}\lambda_{2B}}}{\lambda_{12}\ln(2)} e^{\frac{\lambda_{12}}{2\eta\tau_p\lambda_{1B}\lambda_{2B}}} \times W_{-\frac{1}{2},0}\left(\frac{\lambda_{12}}{\eta\tau_p\lambda_{1B}\lambda_{2B}}\right), \tag{A.10}$$

which is a constant irrelevant to P_s. Summarizing the foregoing results, we can arrive at the scaling behavior of J_1, which completes the proof.

A-2: Asymptotic Behavior of S_2

Firstly, we rewrite S_2 as (A.11), given at the top of the next page. To proceed, with the aid of [30, Eq. (4.331.2)], one can attain (A.12), shown at the top of the next page.

By utilizing the change of variables $t = \frac{P_s z}{\tau_p} - 1$ and $u = \frac{t}{P_s}$, it follows from [30, Eqs. (6.224.1), (4.331.1), and (4.337.2)] that a reformulated expression of S_{221} is given as (A.13) shown in the next page, where $\varpi_8 \triangleq \int_{\sqrt{\frac{\tau_0}{\eta P_s}}}^{\infty} \frac{e^{-\frac{x}{\lambda_{1B}}}\ln\left(1+\frac{\eta\tau_p\lambda_{2B}x}{\lambda_{12}}\right)}{\eta\tau_p\lambda_{2B}x+\lambda_{12}} dx$ and $\varpi_9 \triangleq \frac{1}{\eta\tau_p\lambda_{2B}}\int_{\sqrt{\frac{\tau_0}{\eta P_s}}}^{\infty} \frac{e^{-\frac{x}{\lambda_{1B}}}\ln(x)}{x+\frac{\lambda_{12}}{\eta\tau_p\lambda_{2B}}} dx$. Utilizing [30, Eqs. (3.352.2), (3.351.4), (8.214.1), and (4.331.1)], we have $S_{221} \simeq -\frac{1}{\ln(2)}\left(C_{Euler} + \ln\left(\frac{1}{\eta\lambda_{2B}}\right)\right) - \frac{\lambda_{12}(C_{Euler}-\ln(\lambda_{2B}))}{\eta\tau_p\lambda_{1B}\lambda_{2B}\ln(2)} e^{\frac{\lambda_{12}}{\eta\tau_p\lambda_{1B}\lambda_{2B}}} \mathrm{Ei}\left(-\frac{\lambda_{12}}{\eta\tau_p\lambda_{1B}\lambda_{2B}}\right) +$

$$S_2 \simeq \underbrace{\int_{\frac{\tau_p(\tau_0+1)}{P_s}}^{\infty} f_Z(z) \int_{\sqrt{\frac{\tau_0}{\eta P_s}}}^{\infty} f_X(x) \log_2\left(x\left(\frac{P_s z}{\tau_p}-1\right)\right)\left[e^{-\frac{1}{\lambda_{2B}\eta P_s x}\left(\frac{P_s z}{\tau_p}-1\right)} - e^{-\frac{x}{\lambda_{2B}\tau_0}\left(\frac{P_s z}{\tau_p}-1\right)}\right] dxdz}_{S_{21}}$$
$$- \underbrace{\int_{\frac{\tau_p(\tau_0+1)}{P_s}}^{\infty} f_Z(z) \int_{\sqrt{\frac{\tau_0}{\eta P_s}}}^{\infty} \frac{f_X(x)}{\lambda_{2B}\ln(2)} \int_{\frac{1}{\eta P_s x}\left(\frac{P_s z}{\tau_p}-1\right)}^{\frac{x}{\tau_0}\left(\frac{P_s z}{\tau_p}-1\right)} e^{-\frac{y}{\lambda_{2B}}} \ln(y)\, dydxdz}_{S_{22}}. \tag{A.11}$$

$$S_{22} = \underbrace{\int_{\frac{\tau_p(\tau_0+1)}{P_s}}^{\infty} f_Z(z) \int_{\sqrt{\frac{\tau_0}{\eta P_s}}}^{\infty} \frac{f_X(x)}{\lambda_{2B}\ln(2)}\left[-\lambda_{2B}\mathrm{Ei}\left(-\frac{1}{\lambda_{2B}\eta P_s x}\left(\frac{P_s z}{\tau_p}-1\right)\right) + \lambda_{2B}\ln\left(\frac{\frac{P_s z}{\tau_p}-1}{\eta P_s x}\right) e^{-\frac{\frac{P_s z}{\tau_p}-1}{\lambda_{2B}\eta P_s x}}\right] dxdz}_{S_{221}}$$
$$+ \underbrace{\int_{\frac{\tau_p(\tau_0+1)}{P_s}}^{\infty} f_Z(z) \int_{\sqrt{\frac{\tau_0}{\eta P_s}}}^{\infty} \frac{f_X(x)}{\lambda_{2B}\ln(2)}\left[\lambda_{2B}\mathrm{Ei}\left(-\frac{x}{\lambda_{2B}\tau_0}\left(\frac{P_s z}{\tau_p}-1\right)\right) - \lambda_{2B}\ln\left(\frac{x}{\tau_0}\left(\frac{P_s z}{\tau_p}-1\right)\right) e^{-\frac{x\left(\frac{P_s z}{\tau_p}-1\right)}{\lambda_{2B}\tau_0}}\right] dxdz}_{S_{222}}. \tag{A.12}$$

$$\begin{aligned} S_{221} \simeq & -\frac{1}{\ln(2)} e^{\frac{\lambda_{12}}{\lambda_{1B}\lambda_{2B}\eta\tau_p}} \mathrm{Ei}\left(-\frac{\lambda_{12}}{\lambda_{1B}\lambda_{2B}\eta\tau_p}\right) - \frac{1}{\ln(2)}\left(C_{Euler} + \ln\left(\frac{1}{\eta\lambda_{2B}}\right)\right) + \frac{1}{\ln(2)} e^{\frac{\lambda_{12}}{\eta\tau_p\lambda_{1B}\lambda_{2B}}} \mathrm{Ei}\left(-\frac{\lambda_{12}}{\eta\tau_p\lambda_{1B}\lambda_{2B}}\right) \\ & - \frac{1}{\ln(2)}\left(C_{Euler} + \ln\left(\frac{1}{\lambda_{1B}}\right)\right) - \frac{\lambda_{12}\left(C_{Euler} - \ln(\eta\lambda_{2B})\right)}{\eta\tau_p\lambda_{1B}\lambda_{2B}\ln(2)} e^{\frac{\lambda_{12}}{\eta\tau_p\lambda_{1B}\lambda_{2B}}} \mathrm{Ei}\left(-\frac{1}{\lambda_{1B}}\sqrt{\frac{\tau_0}{\eta P_s}} - \frac{\lambda_{12}}{\eta\tau_p\lambda_{1B}\lambda_{2B}}\right) + \frac{\lambda_{12}}{\lambda_{1B}\ln(2)}\varpi_8 \\ & - \frac{\lambda_{12}}{\lambda_{1B}\ln(2)}\varpi_9 - \frac{1}{\lambda_{1B}\ln(2)} \int_{\sqrt{\frac{\tau_0}{\eta P_s}}}^{\infty} e^{-\frac{x}{\lambda_{1B}}}\left(1 - \frac{\tau_0}{\lambda_{2B}\eta P_s x}\right)\ln(\eta)\, dx + \frac{\lambda_{12}\ln(\eta)}{\lambda_{1B}\ln(2)} \int_{\sqrt{\frac{\tau_0}{\eta P_s}}}^{\infty} \frac{e^{-\frac{x}{\lambda_{1B}}}\left(1 - \frac{\tau_0}{\eta P_s\lambda_{2B}x}\right)}{\tau_p\lambda_{2B}\eta x + \lambda_{12}} dx \\ & - \frac{1}{\lambda_{1B}\ln(2)} \int_{\sqrt{\frac{\tau_0}{\eta P_s}}}^{\infty} e^{-\frac{x}{\lambda_{1B}}}\left(1 - \frac{\tau_0}{\lambda_{2B}\eta P_s x}\right)\ln(x)\, dx + \frac{\lambda_{12}}{\lambda_{1B}\ln(2)} \int_{\sqrt{\frac{\tau_0}{\eta P_s}}}^{\infty} \frac{e^{-\frac{x}{\lambda_{1B}}}\ln(x)}{\tau_p\lambda_{2B}\eta x + \lambda_{12}}\left(1 - \frac{\tau_0}{\lambda_{2B}\eta P_s x}\right) dx, \end{aligned} \tag{A.13}$$

$$S_{222} \simeq \underbrace{-\frac{\tau_p}{\lambda_{12}P_s\ln(2)}\left[\int_{\tau_0}^{\infty} e^{-\frac{\tau_p t}{\lambda_{12}P_s}}\ln\left(t + \frac{\lambda_{2B}\tau_0}{\lambda_{1B}}\right) dt - \int_{\tau_0}^{\infty} e^{-\frac{\tau_p t}{\lambda_{12}P_s}}\ln(t)\, dt\right]}_{S_{222}(\text{Part1})}$$
$$\underbrace{-\frac{\tau_0\tau_p\lambda_{2B}}{\lambda_{12}\lambda_{1B}P_s\ln(2)} e^{\frac{\tau_0\tau_p\lambda_{2B}}{\lambda_{12}\lambda_{1B}P_s}} \int_{\frac{1}{\lambda_{1B}}+\frac{1}{\lambda_{2B}}}^{\infty} e^{-\frac{\tau_0\tau_p\lambda_{2B}}{\lambda_{12}P_s}x}\left[\frac{-C_{\text{Euler}} - \ln(x)}{x} + \frac{\ln\left(\lambda_{2B}\left(x - \frac{1}{\lambda_{1B}}\right)\right)}{x} e^{-\sqrt{\frac{\tau_0}{\eta P_s}}x}\right] dx}_{S_{222}(\text{Part2})}. \tag{A.14}$$

$$S_{21} = \underbrace{\frac{1}{\ln(2)} \int_{\frac{\tau_p(\tau_0+1)}{P_s}}^{\infty} f_Z(z) \int_{\sqrt{\frac{\tau_0}{\eta P_s}}}^{\infty} f_X(x)\left[\ln(x) + \ln\left(\frac{P_s z}{\tau_p}-1\right)\right] e^{-\frac{\frac{P_s z}{\tau_p}-1}{\lambda_{2B}\eta P_s x}} dxdz}_{S_{211}}$$
$$- \underbrace{\frac{1}{\ln(2)} \int_{\frac{\tau_p(\tau_0+1)}{P_s}}^{\infty} f_Z(z) \int_{\sqrt{\frac{\tau_0}{\eta P_s}}}^{\infty} f_X(x)\left[\ln(x) + \ln\left(\frac{P_s z}{\tau_p}-1\right)\right] e^{-\frac{x}{\lambda_{2B}\tau_0}\left(\frac{P_s z}{\tau_p}-1\right)} dxdz}_{S_{212}}. \tag{A.15}$$

$\frac{\lambda_{12}}{\lambda_{1B}\ln(2)}\varpi_8 - \frac{\ln(\eta)}{\ln(2)} \triangleq S_{221}^{\infty}$, where it is clear that S_{221} approaches toward a constant irrelevant to P_s in the high SNR regime. After some algebraic manipulations, S_{222} can be asymptotically written as (A.14), shown in the last page. Next, since $e^{-\frac{\tau_p x}{\lambda_{12}}}\ln\left(1+\frac{\lambda_{2B}\tau_0}{\lambda_{1B}P_s x}\right) \to 0$ at high SNR, we have $S_{222}\left(\text{Part1}\right) = -\frac{\tau_p}{\lambda_{12} ln(2)}\int_{\frac{\tau_0}{P_s}}^{\infty} e^{-\frac{\tau_p x}{\lambda_{12}}} \ln\left(1+\frac{\lambda_{2B}\tau_0}{\lambda_{1B}P_s x}\right)dx \to 0$. For $S_{222}\left(\text{Part2}\right)$, it can be asymptotically written as $S_{222}\left(\text{Part2}\right) \simeq -\frac{\tau_0\tau_p\lambda_{2B}}{\lambda_{12}\lambda_{1B}\ln(2)}\int_{\frac{1}{P_s}\left(\frac{1}{\lambda_{1B}}+\frac{1}{\lambda_{2B}}\right)}^{\infty} e^{-\frac{\tau_0\tau_p\lambda_{2B}t}{\lambda_{12}}}\left[\frac{-C_{Euler}-\ln(P_s t)}{P_s t} + \frac{\ln\left(\lambda_{2B}\left(P_s t-\frac{1}{\lambda_{1B}}\right)\right)}{P_s t}e^{-\sqrt{\frac{\tau_0 P_s}{\eta}}t}\right]dt \to 0$. As a result, we have $S_{22} \simeq S_{221}$. Now, we turn our attention to S_{21}. It follows from (A.11) that S_{21} can be reexpressed as (A.15), given at the bottom of the last page.

For S_{211}, by changing the integration order of dx and dz and invoking the change of variables $u = \frac{P_s z}{\tau_p} - 1$ and $y = \frac{u}{\tau_0}$, $u = \frac{x}{\sqrt{\frac{\tau_0}{\eta P_s}}}$, it follows from [30, Eqs. (4.331.2), (3.352.2), and (8.214.1)] that $S_{211} \simeq \frac{1}{\ln(2)}\left[-C_{Euler}+\ln\left(\lambda_{1B}\right)-\frac{\lambda_{12}}{\eta\tau_p\lambda_{1B}\lambda_{2B}}\varpi_7\right] + \frac{\ln(\tau_0)}{\ln(2)}\left[1+\frac{\lambda_{12}}{\eta\tau_p\lambda_{1B}\lambda_{2B}}e^{\frac{\lambda_{12}}{\eta\tau_p\lambda_{1B}\lambda_{2B}}}\text{Ei}\left(-\frac{\lambda_{12}}{\eta\tau_p\lambda_{1B}\lambda_{2B}}\right)\right] + \left(-\frac{C_{Euler}}{\ln(2)}-\frac{\ln\left(\frac{\tau_0}{P_s}\right)}{\ln(2)}\right)\beta - \frac{\tau_p}{\lambda_{12}\ln(2)}\int_{\sqrt{\frac{\tau_0}{\eta P_s}}}^{\infty} f_X\left(x\right)\frac{\ln\left(\frac{\tau_p}{\lambda_{12}}+\frac{1}{\lambda_{2B}\eta x}\right)}{\frac{\tau_p}{\lambda_{12}}+\frac{1}{\lambda_{2B}\eta x}}dx \propto \log P_s$, where we have $\beta \triangleq 1 + \frac{\lambda_{12}}{\eta\tau_p\lambda_{1B}\lambda_{2B}}e^{\frac{\lambda_{12}}{\eta\tau_p\lambda_{1B}\lambda_{2B}}}\text{Ei}\left(-\frac{\lambda_{12}}{\eta\tau_p\lambda_{1B}\lambda_{2B}}\right)$. On the other hand, by utilizing the L'Hôpital's rule, we have $\lim_{P_s\to\infty} S_{212} = 0$. As a result, we have $S_{21} = S_{211} - S_{212} \simeq S_{211} \propto \log\left(P_s\right)$. Recall that $S_{22} = S_{221} + S_{222} \simeq S_{221}$ at high SNR. As a result, an asymptotic expression of S_2 can be attained.

A-3: Proof of Lemma 3

At high SNR, by utilizing the change of variables $u = \eta x y$ and $v = \frac{\tau_p u}{z}$, it follows from [30, Eq. (4.331.1)] that

$$\epsilon_0 \simeq \frac{-C_{Euler}+\ln\left(\lambda_{2B}\eta x\right)}{\ln\left(2\right)} - \frac{z}{\tau_p\lambda_{2B}\ln\left(2\right)\eta x}\underbrace{\int_1^{\infty} e^{-\frac{z v}{\tau_p\lambda_{2B}\eta x}}\left[\ln\left(\frac{z}{\tau_p}\right)+\ln\left(v\right)\right]dv}_{\sigma}, \tag{A.16}$$

where it follows from [30, Eq. (4.331.2)] that $\sigma = \ln\left(\frac{z}{\tau_p}\right)\frac{\tau_p\lambda_{2B}\eta x}{z}e^{-\frac{z}{\tau_p\lambda_{2B}\eta x}} - \frac{\tau_p\lambda_{2B}\eta x}{z}\text{Ei}\left(-\frac{z}{\tau_p\lambda_{2B}\eta x}\right)$. Next, we define $\epsilon_1 \triangleq \int_0^{\infty} f_X\left(x\right)\epsilon_0 dx$. By invoking [30, Eqs. (4.331.1), (3.471.9) and (6.226.1)], we have

$$\epsilon_1 = \frac{-C_{\text{Euler}}+\ln\left(\lambda_{2B}\eta\right)}{\ln\left(2\right)} - \frac{1}{\ln\left(2\right)}\left[C_{\text{Euler}}-\ln\left(\lambda_{1B}\right)\right] - \frac{2\ln\left(\frac{z}{\tau_p}\right)}{\ln\left(2\right)}\sqrt{\frac{z}{\eta\tau_p\lambda_{1B}\lambda_{2B}}}K_1\left(2\sqrt{\frac{z}{\eta\tau_p\lambda_{1B}\lambda_{2B}}}\right) - \frac{2}{\ln\left(2\right)}K_0\left(\sqrt{\frac{4z}{\eta\tau_p\lambda_{1B}\lambda_{2B}}}\right). \tag{A.17}$$

As a result, at high SNR, by inserting (A.17) into (43) and then by using [30, Eq. (6.614.4)], we complete the proof.

A-4: Asymptotic Behavior of L_2

To begin with, L_2 can be rewritten as (A.18), shown at the top of the next page. After some algebraic manipulations and invoking [30, Eq. (4.331.2)], we have

$$L_{21} = \frac{\ln\left(\frac{P_s x z}{\tau_p}\right)}{\ln\left(2\right)}\left[e^{-\frac{1}{\lambda_{2B}x}\left(\frac{z}{\eta\tau_p}-\frac{1}{\eta P_s}\right)} - e^{-\frac{x}{\tau_0\lambda_{2B}}\left(\frac{P_s z}{\tau_p}-1\right)}\right] - \frac{1}{\ln\left(2\right)}\left\{\frac{1}{\lambda_{2B}}\underbrace{\int_{\frac{1}{x}\left(\frac{z}{\eta\tau_p}-\frac{1}{\eta P_s}\right)}^{\infty} e^{-\frac{y}{\lambda_{2B}}}\ln\left(y\right)dy}_{L_{211}} - \frac{1}{\lambda_{2B}}\underbrace{\int_{\frac{x}{\tau_0}\left(\frac{P_s z}{\tau_p}-1\right)}^{\infty} e^{-\frac{y}{\lambda_{2B}}}\ln\left(y\right)dy}_{L_{212}}\right\}. \tag{A.19}$$

By utilizing the change of variables $u = \frac{y}{\frac{1}{x}\left(\frac{z}{\eta\tau_p}-\frac{1}{\eta P_s}\right)}$ and [30, Eq. (4.331.2)], we have $L_{211} = -\lambda_{2B}\text{Ei}\left(\frac{-1}{x\lambda_{2B}}\left(\frac{z}{\eta\tau_p}-\frac{1}{\eta P_s}\right)\right) + \lambda_{2B}\ln\left(\frac{1}{x}\left(\frac{z}{\eta\tau_p}-\frac{1}{\eta P_s}\right)\right)e^{-\frac{1}{x\lambda_{2B}}\left(\frac{z}{\eta\tau_p}-\frac{1}{\eta P_s}\right)}$. In a similar way, invoking the change of variables $u = \frac{y}{\frac{x}{\tau_0}\left(\frac{P_s z}{\tau_p}-1\right)}$ and [30, Eq. (4.331.2)], we can arrive at $L_{212} = \lambda_{2B}\ln\left(\frac{x}{\tau_0}\left(\frac{P_s z}{\tau_p}-1\right)\right)e^{-\frac{x}{\lambda_{2B}\tau_0}\left(\frac{P_s z}{\tau_p}-1\right)} - \lambda_{2B}\text{Ei}\left(-\frac{x}{\lambda_{2B}\tau_0}\left(\frac{P_s z}{\tau_p}-1\right)\right)$. Summarizing the foregoing results, we can attain a closed-form expression for L_{21}. Then, L_2 can be asymptotically expressed as $L_2 \simeq \int_{\frac{\tau_p}{P_s}}^{\infty} f_Z\left(z\right)\int_{\sqrt{\frac{\tau_0}{\eta P_s}}}^{\infty} f_X\left(x\right)L_{21}dxdz \triangleq \int_{\frac{\tau_p}{P_s}}^{\infty} f_Z\left(z\right)M_1 dz$, in which M_1 can be written as

$$M_1 = \int_{\sqrt{\frac{\tau_0}{\eta P_s}}}^{\infty} f_X\left(x\right)\frac{\ln\left(\frac{P_s x z}{\tau_p}\right)}{\ln(2)}e^{-\frac{1}{\lambda_{2B}x}\left(\frac{z}{\eta\tau_p}-\frac{1}{\eta P_s}\right)}dx - \int_{\sqrt{\frac{\tau_0}{\eta P_s}}}^{\infty} f_X\left(x\right)\frac{\ln\left(\frac{P_s x z}{\tau_p}\right)}{\ln(2)}e^{-\frac{x}{\lambda_{2B}\tau_0}\left(\frac{P_s z}{\tau_p}-1\right)}dx + \frac{1}{\ln(2)}\int_{\sqrt{\frac{\tau_0}{\eta P_s}}}^{\infty} f_X\left(x\right)\text{Ei}\left(\frac{-1}{x\lambda_{2B}}\left(\frac{z}{\eta\tau_p}-\frac{1}{\eta P_s}\right)\right)dx - \frac{1}{\ln(2)}\int_{\sqrt{\frac{\tau_0}{\eta P_s}}}^{\infty} f_X\left(x\right)\ln\left(\frac{1}{x}\left(\frac{z}{\eta\tau_p}-\frac{1}{\eta P_s}\right)\right)e^{-\frac{\frac{z}{\eta\tau_p}-\frac{1}{\eta P_s}}{x\lambda_{2B}}}dx + \frac{1}{\ln(2)}\int_{\sqrt{\frac{\tau_0}{\eta P_s}}}^{\infty} f_X\left(x\right)\ln\left(\frac{x}{\tau_0}\left(\frac{P_s z}{\tau_p}-1\right)\right)e^{-\frac{x}{\lambda_{2B}\tau_0}\left(\frac{P_s z}{\tau_p}-1\right)}dx - \frac{1}{\ln(2)}\int_{\sqrt{\frac{\tau_0}{\eta P_s}}}^{\infty} f_X\left(x\right)\text{Ei}\left(\frac{-x}{\tau_0\lambda_{2B}}\left(\frac{P_s z}{\tau_p}-1\right)\right)dx \triangleq M_{11} - M_{12} + \left(M_{13}-M_{14}+M_{15}-M_{16}\right)/\ln\left(2\right)$. We notice that for M_{11} and M_{14}, it is intractable to attain efficient approximation straightforward. In this case, we jointly consider the outer integration and exchange the integration order to simplify it. For M_{11}, by utilizing the change of variables $u = \frac{z P_s}{\tau_p}$ and [30, Eq. (4.331.2)], we have (A.20), given at the top of the next page, where $\Theta = \frac{-1}{\ln(2)}e^{-\frac{\tau_p}{\lambda_{12}P_s}}\text{Ei}\left(\frac{-1}{\lambda_{1B}}\sqrt{\frac{\tau_0}{\eta P_s}}\right)$. To proceed, we establish the scaling behavior of ϖ_{10} and ϖ_{11}.

Lemma 4: The scaling law of ϖ_{10} and ϖ_{11} is given by

$$\varpi_{10} \propto \log P_s, \varpi_{11} \propto \log P_s. \tag{A.21}$$

Proof: Please refer to Appendix A-5.

Similarly, for M_{14}, by exchanging the integration order and utilizing the change of variables $u = \frac{z}{\eta\tau_p} - \frac{1}{\eta P_s}$, $u = \frac{x}{\sqrt{\frac{\tau_0}{\eta P_s}}}$

$$L_2 \simeq \int_{\frac{\tau_p}{P_s}}^{\infty} f_Z(z) \int_{\sqrt{\frac{\tau_0}{\eta P_s}}}^{\infty} f_X(x) \underbrace{\int_{\frac{1}{x}\left(\frac{z}{\eta\tau_p}-\frac{1}{\eta P_s}\right)}^{\frac{x}{\tau_0}\left(\frac{P_s z}{\tau_p}-1\right)} f_Y(y) \log_2\left(\frac{P_s x z}{\tau_p y}\right) dy}_{L_{21}} dx dz. \tag{A.18}$$

$$\begin{aligned} L_2(M_{11}) &= \int_{\frac{\tau_p}{P_s}}^{\infty} f_Z(z) M_{11} dz \\ &\simeq \frac{1}{\ln(2)} \ln\left(\sqrt{\frac{\tau_0}{\eta P_s}}\right) + \Theta - \frac{\lambda_{12}}{\lambda_{1B}\lambda_{2B}\eta\tau_p \ln(2)} \varpi_7 - \frac{1}{\lambda_{1B}\ln(2)} \underbrace{\int_{\sqrt{\frac{\tau_0}{\eta P_s}}}^{\infty} e^{-\frac{x}{\lambda_{1B}}} \mathrm{Ei}\left(-\frac{\tau_p}{P_s}\left(\frac{1}{\lambda_{12}} + \frac{1}{x\lambda_{2B}\eta\tau_p}\right)\right) dx}_{\varpi_{10}} \\ &+ \frac{\lambda_{12}}{\lambda_{1B}\lambda_{2B}\eta\tau_p \ln(2)} \underbrace{\int_{\sqrt{\frac{\tau_0}{\eta P_s}}}^{\infty} \frac{e^{-\frac{x}{\lambda_{1B}}}}{x + \frac{\lambda_{12}}{\lambda_{2B}\eta\tau_p}} \mathrm{Ei}\left(-\frac{\tau_p}{P_s}\left(\frac{1}{\lambda_{12}} + \frac{1}{x\lambda_{2B}\eta\tau_p}\right)\right) dx}_{\varpi_{11}}, \end{aligned} \tag{A.20}$$

and [30, Eqs. (4.331.1) and (3.352.2)], we have

$$\begin{aligned} L_2(M_{14}) \simeq{}& \frac{C_{\mathrm{Euler}}}{\ln(2)} + \frac{\lambda_{12} C_{\mathrm{Euler}} e^{\frac{\lambda_{12}}{\lambda_{1B}\lambda_{2B}\eta\tau_p}} \mathrm{Ei}\left(-\frac{\lambda_{12}}{\lambda_{1B}\lambda_{2B}\eta\tau_p}\right)}{\lambda_{1B}\lambda_{2B}\eta\tau_p \ln(2)} \\ &+ \frac{\varpi_{12}}{\lambda_{1B}\ln(2)} - \frac{\lambda_{12}}{\lambda_{1B}\lambda_{2B}\eta\tau_p\ln(2)}\varpi_{13} \\ &+ \frac{\ln\left(\sqrt{\frac{\tau_0}{\eta P_s}}\right)}{\ln(2)} + \Theta^{\infty} - \frac{\lambda_{12}}{\lambda_{1B}\lambda_{2B}\eta\tau_p\ln(2)}\varpi_7, \end{aligned} \tag{A.22}$$

where $\varpi_{12} = \int_{\sqrt{\frac{\tau_0}{\eta P_s}}}^{\infty} e^{-\frac{x}{\lambda_{1B}}} \ln\left(\frac{\eta\tau_p}{\lambda_{12}} + \frac{1}{x\lambda_{2B}}\right) dx$, $\varpi_{13} = \int_{\sqrt{\frac{\tau_0}{\eta P_s}}}^{\infty} \frac{e^{-\frac{x}{\lambda_{1B}}}}{x + \frac{\lambda_{12}}{\lambda_{2B}\eta\tau_p}} \ln\left(\frac{\eta\tau_p}{\lambda_{12}} + \frac{1}{x\lambda_{2B}}\right) dx$, and Θ^{∞} is given by $\Theta^{\infty} = -\frac{1}{\ln(2)}\left[C_{Euler} + \ln\left(\frac{1}{\lambda_{1B}}\sqrt{\frac{\tau_0}{\eta P_s}}\right)\right] \propto \log P_s$. Since ϖ_{11}, ϖ_{12}, and ϖ_{13} approaches to constants at high SNR, we have $L_2(M_{14}) \propto \log(P_s)$. Next, we concentrate on the analysis of M_{12}. Invoking the change of variables $u = \frac{x}{\sqrt{\frac{\tau_0}{\eta P_s}}}$ and utilizing [30, Eq. (4.331.2)], one can attain (A.23), given at the top of the next page. Next, by invoking the change of variables $u = \frac{P_s z}{\tau_p} - 1$ and $x = 1 + u$, R_1 can be asymptotically expressed as

$$\begin{aligned} R_1 \simeq{}& -\frac{\tau_p e^{\left(\frac{1}{\lambda_{2B}\tau_0} - \frac{1}{\lambda_{1B}}\right)\sqrt{\frac{\tau_0}{\eta P_s}}}}{\lambda_{12}\lambda_{1B}P_s\ln(2)} (\lambda_{2B}\tau_0) \\ &\times \underbrace{\int_1^{\infty} \frac{\ln(x) e^{-x\left(\frac{\tau_p}{\lambda_{12}P_s} + \frac{1}{\lambda_{2B}\tau_0}\sqrt{\frac{\tau_0}{\eta P_s}}\right)}}{x + \lambda_{2B}\tau_0\left(\frac{1}{\lambda_{1B}} - \frac{1}{\lambda_{2B}\tau_0}\right)} dx}_{\varpi_{14}}, \end{aligned} \tag{A.24}$$

where in the case of $\frac{\lambda_{2B}\tau_0}{\lambda_{1B}} - 1 = 1$, a closed-form expression of ϖ_{14} can be given as $\varpi_{14} = \frac{1}{2} e^{\frac{\tau_p}{\lambda_{12}P_s} + \frac{1}{\lambda_{2B}\tau_0}\sqrt{\frac{\tau_0}{\eta P_s}}} \left[\mathrm{Ei}\left(-\frac{\tau_p}{\lambda_{12}P_s} - \frac{1}{\lambda_{2B}\tau_0}\sqrt{\frac{\tau_0}{\eta P_s}}\right)\right]^2$. In the general case, at high SNR, we have $\varpi_{14} \simeq \varpi_{15} + \ln(P_s)\left[-\frac{C_{Euler}}{2} + \frac{\ln\left(\lambda_{2B}\sqrt{\eta\tau_0}\right)}{2}\right] + \frac{1}{4}[\ln(P_s)]^2 \propto [\log(P_s)]^2$, where we define $\varpi_{15} \triangleq \int_{\frac{1}{\sqrt{P_s}}}^{\infty} \frac{\ln(t)}{t} e^{-\frac{t}{\lambda_{2B}\sqrt{\eta\tau_0}}} dt \propto [\log(P_s)]^2$. The detailed derivation of ϖ_{14} at high SNR is provided in Appendix A-6. By its turn, R_1 can be asymptotically expressed as

$$R_1 \simeq -\frac{\tau_0\tau_p\lambda_{2B}}{\lambda_{12}\lambda_{1B}P_s\ln(2)}\varpi_{14} \propto \frac{[\log(P_s)]^2}{P_s} \to 0. \tag{A.25}$$

For R_2, invoking the change of variables $u = \frac{P_s z}{\tau_p} - 1$ and [30, Eq. (3.352.4)], we have

$$\begin{aligned} R_2 &\simeq \frac{\lambda_{2B}\tau_0\tau_p \ln\left(\frac{\tau_0}{\eta P_s}\right)}{2\lambda_{12}\lambda_{1B}P_s\ln(2)} \left[C_{Euler} + \ln\left(\frac{\sqrt{\frac{\tau_0}{\eta P_s}}}{\lambda_{1B}}\right)\right] \\ &\propto \frac{[\ln(P_s)]^2}{P_s} \to 0. \end{aligned} \tag{A.26}$$

For R_3, one can attain

$$\begin{aligned} R_3 = \frac{\lambda_{2B}\tau_0\tau_p}{\lambda_{12}\lambda_{1B}P_s\ln(2)} e^{-\frac{\tau_p}{\lambda_{12}P_s}} \\ \times \underbrace{\int_0^{\infty} \frac{e^{-\frac{\tau_p u}{\lambda_{12}P_s}} \mathrm{Ei}\left(-\sqrt{\frac{\tau_0}{\eta P_s}}\left(\frac{1}{\lambda_{1B}} + \frac{u}{\lambda_{2B}\tau_0}\right)\right)}{u + \frac{\lambda_{2B}\tau_0}{\lambda_{1B}}} du}_{\varpi_{16}}, \end{aligned} \tag{A.27}$$

where we have $\varpi_{16} \propto [\log(P_s)]^2$. The proof of the scaling law of ϖ_{16} is provided in Appendix A-7. By its turn, we have $R_3 \propto \frac{[\log(P_s)]^2}{P_s} \to 0$, which leads to $L_2(M_{12}) \propto \frac{[\log(P_s)]^2}{P_s}$.

For M_{13}, utilizing the change of variables $u = \frac{\lambda_{2B}x}{4\left(\frac{z}{\eta\tau_p} - \frac{1}{\eta P_s}\right)}$ and [30, Eq. (6.226.1)], one can attain $M_{13} \simeq \frac{1}{\lambda_{1B}}\int_0^{\infty} e^{-\frac{x}{\lambda_{1B}}} \mathrm{Ei}\left(-\frac{1}{x\lambda_{2B}}\left(\frac{z}{\eta\tau_p} - \frac{1}{\eta P_s}\right)\right) dx \simeq -2K_0\left(\sqrt{\frac{4\left(\frac{z}{\eta\tau_p} - \frac{1}{\eta P_s}\right)}{\lambda_{1B}\lambda_{2B}}}\right)$. Next, for $L_2(M_{13})$, making use of the change of variables $u = \frac{z}{\eta\tau_p} - \frac{1}{\eta P_s}$ and [30, Eq. (6.614.4)],

$$L_2\left(M_{12}\right) \simeq \underbrace{-\frac{1}{\lambda_{1B}\ln\left(2\right)}\int_{\frac{\tau_p}{P_s}}^{\infty} f_Z\left(z\right)\ln\left(\frac{P_s z}{\tau_p}\right)\frac{e^{-\sqrt{\frac{\tau_0}{\eta P_s}}\left(\frac{1}{\lambda_{1B}}+\frac{\frac{P_s z}{\tau_p}-1}{\lambda_{2B}\tau_0}\right)}}{\frac{1}{\lambda_{1B}}+\frac{\frac{P_s z}{\tau_p}-1}{\lambda_{2B}\tau_0}}dz}_{R_1} \underbrace{-\frac{\sqrt{\frac{\tau_0}{\eta P_s}}}{\lambda_{1B}\ln\left(2\right)}\int_{\frac{\tau_p}{P_s}}^{\infty} f_Z\left(z\right)\ln\left(\sqrt{\frac{\tau_0}{\eta P_s}}\right)\frac{e^{-\sqrt{\frac{\tau_0}{\eta P_s}}\left[\frac{1}{\lambda_{1B}}+\frac{1}{\lambda_{2B}\tau_0}\left(\frac{P_s z}{\tau_p}-1\right)\right]}}{\sqrt{\frac{\tau_0}{\eta P_s}}\left[\frac{1}{\lambda_{1B}}+\frac{1}{\lambda_{2B}\tau_0}\left(\frac{P_s z}{\tau_p}-1\right)\right]}dz}_{R_2}$$
$$+\underbrace{\frac{\sqrt{\frac{\tau_0}{\eta P_s}}}{\lambda_{1B}\ln\left(2\right)}\int_{\frac{\tau_p}{P_s}}^{\infty} f_Z\left(z\right)\frac{\mathrm{Ei}\left(-\sqrt{\frac{\tau_0}{\eta P_s}}\left(\frac{1}{\lambda_{1B}}+\frac{1}{\lambda_{2B}\tau_0}\left(\frac{P_s z}{\tau_p}-1\right)\right)\right)}{\sqrt{\frac{\tau_0}{\eta P_s}}\left[\frac{1}{\lambda_{1B}}+\frac{1}{\lambda_{2B}\tau_0}\left(\frac{P_s z}{\tau_p}-1\right)\right]}dz}_{R_3}. \quad \text{(A.23)}$$

we have

$$L_2\left(M_{13}\right) \simeq -\frac{e^{\frac{\lambda_{12}}{2\eta\tau_p\lambda_{1B}\lambda_{2B}}}}{\ln\left(2\right)} \times\sqrt{\frac{\eta\tau_p\lambda_{1B}\lambda_{2B}}{\lambda_{12}}}W_{-0.5,0}\left(\frac{\lambda_{12}}{\eta\tau_p\lambda_{1B}\lambda_{2B}}\right). \quad \text{(A.28)}$$

For M_{15}, by utilizing the change of variables $u=\frac{x}{\sqrt{\frac{\tau_0}{\eta P_s}}}$ and using [30, Eq. (4.331.2)], we have $M_{15} \simeq \frac{-1}{1+\frac{\lambda_{1B}}{\lambda_{2B}\tau_0}\left(\frac{P_s z}{\tau_p}-1\right)}\mathrm{Ei}\left(-\sqrt{\frac{\tau_0}{\eta P_s}}\left(\frac{1}{\lambda_{1B}}+\frac{1}{\lambda_{2B}\tau_0}\left(\frac{P_s z}{\tau_p}-1\right)\right)\right) + \ln\left(\sqrt{\frac{\tau_0}{\eta P_s}}\right)\frac{e^{-\sqrt{\frac{\tau_0}{\eta P_s}}\left[\frac{1}{\lambda_{1B}}+\frac{1}{\lambda_{2B}\tau_0}\left(\frac{P_s z}{\tau_p}-1\right)\right]}}{1+\frac{\lambda_{1B}}{\lambda_{2B}\tau_0}\left(\frac{P_s z}{\tau_p}-1\right)} + \frac{\ln\left(\frac{1}{\tau_0}\left(\frac{P_s z}{\tau_p}-1\right)\right)e^{-\sqrt{\frac{\tau_0}{\eta P_s}}\left[\frac{1}{\lambda_{1B}}+\frac{1}{\lambda_{2B}\tau_0}\left(\frac{P_s z}{\tau_p}-1\right)\right]}}{1+\frac{\lambda_{1B}}{\lambda_{2B}\tau_0}\left(\frac{P_s z}{\tau_p}-1\right)}$. Accordingly, by examining the outer-layer integration for M_{15} and invoking the change of variables $u=\frac{P_s z}{\tau_p}-1$, it follows from [30, Eq. (3.352.4)] that

$$L_2\left(M_{15}\right) \simeq -\frac{\tau_p e^{-\frac{\tau_p}{\lambda_{12}P_s}}}{\lambda_{12}P_s\ln\left(2\right)}\frac{\lambda_{2B}\tau_0}{\lambda_{1B}}\varpi_{14} + \frac{\tau_p\ln\left(\sqrt{\frac{\tau_0}{\eta P_s}}\right)}{\lambda_{12}P_s\ln\left(2\right)}e^{-\frac{1}{\lambda_{1B}}\sqrt{\frac{\tau_0}{\eta P_s}}-\frac{\tau_p}{\lambda_{12}P_s}}Q_1 + \frac{\tau_p}{\lambda_{12}P_s\ln\left(2\right)}e^{-\frac{1}{\lambda_{1B}}\sqrt{\frac{\tau_0}{\eta P_s}}-\frac{\tau_p}{\lambda_{12}P_s}}Q_2, \quad \text{(A.29)}$$

where we have

$$Q_1 = -\frac{\lambda_{2B}\tau_0}{\lambda_{1B}}e^{\frac{\lambda_{2B}\tau_0}{\lambda_{1B}}\left(\frac{\tau_p}{\lambda_{12}P_s}+\frac{\sqrt{\frac{\tau_0}{\eta P_s}}}{\lambda_{2B}\tau_0}\right)} \times\mathrm{Ei}\left(-\frac{\lambda_{2B}\tau_0}{\lambda_{1B}}\left(\frac{\tau_p}{\lambda_{12}P_s}+\frac{\sqrt{\frac{\tau_0}{\eta P_s}}}{\lambda_{2B}\tau_0}\right)\right), \quad \text{(A.30)}$$

$$Q_2 = \frac{\lambda_{2B}\tau_0}{\lambda_{1B}}\varpi_{17}+\frac{\lambda_{2B}\tau_0}{\lambda_{1B}}\ln\left(\tau_0\right)e^{\frac{\lambda_{2B}\tau_0}{\lambda_{1B}}\left(\frac{\tau_p}{\lambda_{12}P_s}+\frac{\sqrt{\frac{\tau_0}{\eta P_s}}}{\lambda_{2B}\tau_0}\right)} \times\mathrm{Ei}\left(-\frac{\lambda_{2B}\tau_0}{\lambda_{1B}}\left(\frac{\tau_p}{\lambda_{12}P_s}+\frac{\sqrt{\frac{\tau_0}{\eta P_s}}}{\lambda_{2B}\tau_0}\right)\right), \quad \text{(A.31)}$$

in which we have defined $\varpi_{17} = \int_0^{\infty}\ln\left(u\right)e^{-u\left(\frac{\tau_p}{\lambda_{12}P_s}+\frac{\sqrt{\frac{\tau_0}{\eta P_s}}}{\lambda_{2B}\tau_0}\right)}/\left(u+\frac{\lambda_{2B}\tau_0}{\lambda_{1B}}\right)du$.

Next, we focus on the asymptotic behavior of Q_1 and Q_2. Firstly, Q_1 can be expressed as $Q_1 \simeq -\frac{\lambda_{2B}\tau_0}{\lambda_{1B}}\left[C_{Euler}+\ln\left(\frac{\lambda_{2B}\tau_0}{\lambda_{1B}}\left(\frac{\tau_p}{\lambda_{12}P_s}+\frac{\sqrt{\frac{\tau_0}{\eta P_s}}}{\lambda_{2B}\tau_0}\right)\right)\right] \propto \log P_s$. Next, based on the derivation given in Appendix A-8, at high SNR, we have $\varpi_{17} \propto \left[\log\left(P_s\right)\right]^2$, based on which one can readily show that $Q_2 \propto \left[\log\left(P_s\right)\right]^2$. As a result, we can arrive at $L_2\left(M_{15}\right) \propto \frac{\left[\log(P_s)\right]^2}{P_s}$.

Finally, let us focus on M_{16}. At high SNR, by making use of [30, Eq. (6.224.1)], M_{16} can be asymptotically written as $M_{16} \simeq -\ln\left(1+\frac{1}{\lambda_{1B}}\frac{\lambda_{2B}\tau_0}{\frac{P_s z}{\tau_p}-1}\right)$. By its turn, we can attain $L_2\left(M_{16}\right) \simeq \lim_{u\to 0}\ln\left(1+\frac{\lambda_{2B}\tau_0}{\lambda_{1B}u}\right)/\ln\left(2\right) + \lim_{t\to 0}\left[C_{Euler}+\ln\left(\frac{\tau_p t}{\lambda_{12}P_s}\right)\right]/\ln\left(2\right) - \left[C_{Euler}+\ln\left(\frac{\tau_0\tau_p\lambda_{2B}}{\lambda_{12}\lambda_{1B}P_s}\right)\right]/\ln\left(2\right) = \lim_{u\to 0}\ln\left(1+\frac{\lambda_{2B}\tau_0}{\lambda_{1B}u}\right)/\ln\left(2\right) + \lim_{t\to 0}\ln\left(\frac{\lambda_{1B}t}{\lambda_{2B}\tau_0}\right)/\ln\left(2\right) \to 0$. To summarize, L_2 can be asymptotically written as $L_2 \simeq L_2\left(M_{11}\right)+L_2\left(M_{13}\right)+L_2\left(M_{14}\right) \propto \log\left(P_s\right)$. This completes the derivations.

A-5: Asymptotic Behavior of ϖ_{10} and ϖ_{11}

With the aid of [30, Eq. (8.214.1)], ϖ_{10} can be asymptotically expressed as

$$\varpi_{10} \simeq C_{Euler}\lambda_{1B}+\ln\left(\frac{\tau_p}{P_s}\right)\lambda_{1B} + \underbrace{\int_{\sqrt{\frac{\tau_0}{\eta P_s}}}^{\infty} e^{-\frac{x}{\lambda_{1B}}}\ln\left(\frac{1}{\lambda_{12}}+\frac{1}{x\lambda_{2B}\eta\tau_p}\right)dx}_{\varpi_{19}} \propto \log P_s, \quad \text{(A.32)}$$

where ϖ_{19} approaches to a constant in the high SNR regions. For ϖ_{11}, it follows from [30, Eqs. (8.214.1) and (3.352.2)] that $\varpi_{11} \simeq \int_{\sqrt{\frac{\tau_0}{\eta P_s}}}^{\infty}\frac{e^{-\frac{x}{\lambda_{1B}}}}{x+\frac{\lambda_{12}}{\lambda_{2B}\eta\tau_p}}\left[C_{Euler}+\ln\left(\frac{\tau_p}{P_s}\left(\frac{1}{\lambda_{12}}+\frac{1}{x\lambda_{2B}\eta\tau_p}\right)\right)\right]dx \simeq -\left(C_{Euler}+\ln\left(\frac{\tau_p}{P_s}\right)-\ln\left(\eta\tau_p\right)\right)e^{\frac{\lambda_{12}}{\lambda_{1B}\lambda_{2B}\eta\tau_p}}\mathrm{Ei}\left(-\frac{\lambda_{12}}{\lambda_{1B}\lambda_{2B}\eta\tau_p}\right)+\varpi_{13} \propto \log P_s$.

A-6: Asymptotic Analysis of ϖ_{14}

Firstly, ϖ_{14} can be asymptotically expressed as $\varpi_{14} \simeq \int_1^{\infty}\frac{\ln(x)e^{-x\left(\frac{1}{\lambda_{2B}\tau_0}\sqrt{\frac{\tau_0}{\eta P_s}}\right)}}{x+\lambda_{2B}\tau_0\left(\frac{1}{\lambda_{1B}}-\frac{1}{\lambda_{2B}\tau_0}\right)}dx$. By defining $t=\frac{x}{\sqrt{P_s}}$, we

have $\varpi_{14} \simeq \int_{\frac{1}{\sqrt{P_s}}}^{\infty} \frac{\left[\ln(t)+\ln\left(\sqrt{P_s}\right)\right]e^{-\frac{t}{\lambda_{2B}\tau_0}\sqrt{\frac{\tau_0}{\eta}}}}{t+\frac{\lambda_{2B}\tau_0\left(\frac{1}{\lambda_{1B}}-\frac{1}{\lambda_{2B}\tau_0}\right)}{\sqrt{P_s}}} dt$. With the aid of [30, Eqs. (3.381.6) and (8.211.1)], we have $\varpi_{14} \simeq \int_{\frac{1}{\sqrt{P_s}}}^{\infty} \frac{\ln(t)}{t} e^{-\frac{t}{\lambda_{2B}\sqrt{\eta\tau_0}}} dt - \ln\left(\sqrt{P_s}\right) \mathrm{Ei}\left(-\frac{1}{\lambda_{2B}\sqrt{\eta\tau_0 P_s}}\right)$. Next, by invoking [30, Eq. (8.214.1)] and after some algebraic manipulations, we can complete the derivation.

A-7: Asymptotic Behavior of ϖ_{16}

To begin with, one can arrive at $\varpi_{16} = e^{\frac{\tau_0\tau_p\lambda_{2B}}{\lambda_{12}\lambda_{1B}P_s}} \int_{\frac{\lambda_{2B}\tau_0}{\lambda_{1B}}}^{\infty} \frac{e^{-\frac{\tau_p}{\lambda_{12}P_s}x}}{x} \mathrm{Ei}\left(-\sqrt{\frac{\tau_0}{\eta P_s}}\frac{x}{\lambda_{2B}\tau_0}\right)dx \simeq \int_{\frac{\lambda_{2B}\tau_0}{\lambda_{1B}}}^{\infty} \frac{e^{-\frac{\tau_p}{\lambda_{12}P_s}x}}{x} \mathrm{Ei}\left(-\sqrt{\frac{\tau_0}{\eta P_s}}\frac{x}{\lambda_{2B}\tau_0}\right)dx \triangleq \varpi_{18}$ by invoking the change of variables $x = u + \frac{\lambda_{2B}\tau_0}{\lambda_{1B}}$. Equivalently, ϖ_{18} can be rewritten as $\varpi_{18} = -\int_{\frac{\lambda_{2B}\tau_0}{\lambda_{1B}}}^{\infty} \frac{e^{-\frac{\tau_p}{\lambda_{12}P_s}x}}{x} E_1\left(\sqrt{\frac{\tau_0}{\eta P_s}}\frac{x}{\lambda_{2B}\tau_0}\right)dx > -\int_{\frac{\lambda_{2B}\tau_0}{\lambda_{1B}}}^{\infty} \frac{e^{-\frac{\tau_p}{\lambda_{12}P_s}x-\sqrt{\frac{\tau_0}{\eta P_s}}\frac{x}{\lambda_{2B}\tau_0}}}{x} \ln\left(1+\frac{1}{\sqrt{\frac{\tau_0}{\eta P_s}}\frac{x}{\lambda_{2B}\tau_0}}\right)dx \triangleq \varpi_{18}^{LB}$, where ϖ_{18}^{LB} is a tight lower bound and will be used to characterize the scaling behavior of ϖ_{18} (or equivalently, ϖ_{16}). Making use of the change of variables $t = \sqrt{\frac{\tau_0}{\eta P_s}}\frac{x}{\lambda_{2B}\tau_0}$, we have $\varpi_{18}^{LB} = -\int_{\frac{1}{\lambda_{1B}}\sqrt{\frac{\tau_0}{\eta P_s}}}^{\infty} \frac{e^{-t}}{t}\ln\left(1+\frac{1}{t}\right)dt$. Then, it follows that $\lim_{P_s\to\infty} \frac{\varpi_{18}^{LB}}{[\ln(P_s)]^2} = -\frac{1}{8}$, which completes the proof.

A-8: Asymptotic Behavior of ϖ_{17}

For sufficiently high SNR, ϖ_{17} can be asymptotically written as $\varpi_{17} \simeq \int_0^{\infty} \frac{e^{-u\frac{\sqrt{\frac{\tau_0}{\eta P_s}}}{\lambda_{2B}\tau_0}}}{u+\frac{\lambda_{2B}\tau_0}{\lambda_{1B}}}\ln(u)\,du$. By using the change of variables $x = \frac{u}{\sqrt{P_s}}$, it follows that

$$\varpi_{17} \simeq \underbrace{\frac{1}{2}\ln(P_s)\int_0^{\infty} \frac{e^{-x\frac{\sqrt{\frac{\tau_0}{\eta}}}{\lambda_{2B}\tau_0}}}{x+\frac{\lambda_{2B}\tau_0}{\lambda_{1B}\sqrt{P_s}}}dx}_{\varpi_{17}^{(1)}} + \underbrace{\int_0^{\infty} \frac{e^{-x\frac{\sqrt{\frac{\tau_0}{\eta}}}{\lambda_{2B}\tau_0}}\ln(x)}{x+\frac{\lambda_{2B}\tau_0}{\lambda_{1B}\sqrt{P_s}}}dx}_{\varpi_{17}^{(2)}}. \tag{A.33}$$

For $\varpi_{17}^{(1)}$, utilizing [30, Eq. (3.352.4)], we have $\varpi_{17}^{(1)} = -\frac{1}{2}\ln(P_s)\, e^{\frac{1}{\lambda_{1B}}\sqrt{\frac{\tau_0}{\eta P_s}}} \mathrm{Ei}\left(-\frac{1}{\lambda_{1B}}\sqrt{\frac{\tau_0}{\eta P_s}}\right) \simeq -\frac{1}{2}\ln(P_s)\left[C_{Euler}+\ln\left(\frac{1}{\lambda_{1B}}\sqrt{\frac{\tau_0}{\eta P_s}}\right)\right] \propto [\log(P_s)]^2$. On the other hand, for $\varpi_{17}^{(2)}$, invoking the change of variables $t = x + \frac{\lambda_{2B}\tau_0}{\lambda_{1B}\sqrt{P_s}}$, we have $\varpi_{17}^{(2)} = \int_{\frac{\lambda_{2B}\tau_0}{\lambda_{1B}\sqrt{P_s}}}^{\infty} \frac{e^{-\frac{\sqrt{\frac{\tau_0}{\eta}}}{\lambda_{2B}\tau_0}\left(t-\frac{\lambda_{2B}\tau_0}{\lambda_{1B}\sqrt{P_s}}\right)}}{t}\ln\left(t-\frac{\lambda_{2B}\tau_0}{\lambda_{1B}\sqrt{P_s}}\right)dt \simeq \int_{\frac{\lambda_{2B}\tau_0}{\lambda_{1B}\sqrt{P_s}}}^{\infty} \frac{e^{-\frac{\sqrt{\frac{\tau_0}{\eta}}}{\lambda_{2B}\tau_0}t}}{t}\ln(t)\,dt$. Finally, it follows that $\lim_{P_s\to\infty} \frac{\varpi_{17}^{(2)}}{[\ln(P_s)]^2} = -\frac{1}{8}$. This by its turn leads to $\varpi_{17} \propto [\log(P_s)]^2$, which completes the proof.

A-9: Proof of Proposition 8

To prove the equivalence of the two asymptotic expressions, we rewrite the last term of (39) as $\wp = -\frac{1}{\lambda_{1B}\ln(2)}\int_{\sqrt{\frac{\tau_0}{\eta P_s}}}^{\infty} e^{-\frac{x}{\lambda_{1B}}}\ln\left(1+\frac{\eta\tau_p\lambda_{2B}x}{\lambda_{12}}\right)dx + \frac{\lambda_{12}}{\lambda_{1B}\ln(2)}\int_{\sqrt{\frac{\tau_0}{\eta P_s}}}^{\infty} e^{-\frac{x}{\lambda_{1B}}}\frac{\ln\left(1+\frac{\eta\tau_p\lambda_{2B}x}{\lambda_{12}}\right)}{\lambda_{12}+\eta\tau_p\lambda_{2B}x}dx + \frac{\ln(\lambda_{2B}\eta)}{\lambda_{1B}\ln(2)}\int_{\sqrt{\frac{\tau_0}{\eta P_s}}}^{\infty} e^{-\frac{x}{\lambda_{1B}}}\left(1-\frac{\lambda_{12}}{\lambda_{12}+\eta\tau_p\lambda_{2B}x}\right)dx + \frac{1}{\lambda_{1B}\ln(2)}\int_{\sqrt{\frac{\tau_0}{\eta P_s}}}^{\infty} e^{-\frac{x}{\lambda_{1B}}}\left(1-\frac{\lambda_{12}}{\lambda_{12}+\eta\tau_p\lambda_{2B}x}\right)\ln(x)\,dx$. Invoking the change of variables $t = 1 + \frac{\eta\tau_p\lambda_{2B}x}{\lambda_{12}}$ and [30, Eq. (4.331.1)], one can show that $\wp \simeq -\frac{\lambda_{12}e^{\frac{\lambda_{12}}{\eta\tau_p\lambda_{1B}\lambda_{2B}}}}{\eta\tau_p\lambda_{1B}\lambda_{2B}\ln(2)}\int_1^{\infty} e^{-\frac{\lambda_{12}}{\eta\tau_p\lambda_{1B}\lambda_{2B}}t}\ln(t)\,dt + \frac{\lambda_{12}}{\lambda_{1B}\ln(2)}\varpi_8 + \frac{\ln(\lambda_{2B}\eta)}{\ln(2)} - \frac{\lambda_{12}\ln(\lambda_{2B}\eta)}{\eta\tau_p\lambda_{1B}\lambda_{2B}\ln(2)}\int_{\sqrt{\frac{\tau_0}{\eta P_s}}}^{\infty} \frac{e^{-\frac{x}{\lambda_{1B}}}}{x+\frac{\lambda_{12}}{\eta\tau_p\lambda_{2B}}}dx - \frac{C_{Euler}-\ln(\lambda_{1B})}{\ln(2)} - \frac{\lambda_{12}}{\eta\tau_p\lambda_{1B}\lambda_{2B}\ln(2)}\varpi_7$. Making use of [30, Eqs. (4.331.2) and (3.352.2)], we have

$$\begin{aligned}\wp \simeq\ & \frac{\lambda_{12}\ln(\lambda_{2B}\eta)\, e^{\frac{\lambda_{12}}{\eta\tau_p\lambda_{1B}\lambda_{2B}}}}{\eta\tau_p\lambda_{1B}\lambda_{2B}\ln(2)} \\ & \times \mathrm{Ei}\left(-\frac{\lambda_{12}}{\eta\tau_p\lambda_{1B}\lambda_{2B}}\right) - \frac{C_{Euler}-\ln(\lambda_{1B})}{\ln(2)} \\ & - \frac{\lambda_{12}}{\eta\tau_p\lambda_{1B}\lambda_{2B}\ln(2)}\varpi_7 + \frac{e^{\frac{\lambda_{12}}{\eta\tau_p\lambda_{1B}\lambda_{2B}}}}{\ln(2)}\mathrm{Ei}\left(-\frac{\lambda_{12}}{\eta\tau_p\lambda_{1B}\lambda_{2B}}\right) \\ & + \frac{\lambda_{12}}{\lambda_{1B}\ln(2)}\varpi_8 + \frac{\ln(\lambda_{2B}\eta)}{\ln(2)}.\end{aligned} \tag{A.34}$$

Now, by plugging (A.34) into (39) and after some algebraic manipulations, one can arrive at

$$\begin{aligned}C_{BC,T_{1,c}} \simeq\ & \frac{\ln(P_s)}{\ln(2)} + \frac{2\left(\ln(\lambda_{1B}) - C_{Euler}\right)}{\ln(2)} \\ & + \frac{e^{\frac{\lambda_{12}}{\eta\tau_p\lambda_{1B}\lambda_{2B}}}}{\ln(2)}\mathrm{Ei}\left(-\frac{\lambda_{12}}{\eta\tau_p\lambda_{1B}\lambda_{2B}}\right) + \frac{\ln(\eta)}{\ln(2)}.\end{aligned} \tag{A.35}$$

Recall that for the scenario where T2 is not required to decode $c(n)$, the ergodic capacity of the backscatter link T1-BD-T1 can be asymptotically expressed as

$$\begin{aligned}C_{BC,T_1} \simeq\ & \frac{\ln(P_s)}{\ln(2)} + \frac{2\left(\ln(\lambda_{1B}) - C_{Euler}\right) + \ln(\eta)}{\ln(2)} \\ & - \frac{e^{\frac{\lambda_{12}}{2\eta\tau_p\lambda_{1B}\lambda_{2B}}}}{\ln(2)}\sqrt{\frac{\eta\tau_p\lambda_{1B}\lambda_{2B}}{\lambda_{12}}}W_{-0.5,0}\left(\frac{\lambda_{12}}{\eta\tau_p\lambda_{1B}\lambda_{2B}}\right).\end{aligned} \tag{A.36}$$

Finally, utilizing the definitions of $\mathrm{Ei}(\cdot)$ and $W_{a,b}(\cdot)$ [30, Eqs. (9.222.1) and (8.211.1)], one can attain $e^{\frac{\lambda_{12}}{2\eta\tau_p\lambda_{1B}\lambda_{2B}}}\mathrm{Ei}\left(-\frac{\lambda_{12}}{\eta\tau_p\lambda_{1B}\lambda_{2B}}\right) = -\sqrt{\frac{\eta\tau_p\lambda_{1B}\lambda_{2B}}{\lambda_{12}}}W_{-0.5,0}\left(\frac{\lambda_{12}}{\eta\tau_p\lambda_{1B}\lambda_{2B}}\right)$, which leads to the fact that (A.35) is equal to (A.36). This completes the proof.

REFERENCES

[1] K. Han and K. Huang, "Wirelessly powered backscatter communication networks: Modeling, coverage, and capacity," *IEEE Trans. Wireless Commun.*, vol. 16, no. 4, pp. 2548–2561, 2017.

[2] N. Van Huynh, D. T. Hoang, X. Lu, D. Niyato, P. Wang, and D. I. Kim, "Ambient backscatter communications: A contemporary survey," *IEEE Commun. Surveys Tuts.*, vol. 20, no. 4, pp. 2889–2922, Fourthquarter 2018.

[3] H. Guo, Y. Liang, R. Long, S. Xiao, and Q. Zhang, "Resource allocation for symbiotic radio system with fading channels," *IEEE Access*, vol. 7, pp. 34 333–34 347, 2019.

[4] S. T. Shah, K. W. Choi, T. J. Lee, and M. Y. Chung, "Outage probability and throughput analysis of SWIPT enabled cognitive relay network with ambient backscatter," *IEEE Internet Things J.*, vol. 5, no. 4, pp. 3198–3208, 2018.

[5] V. Liu, A. Parks, V. Talla, S. Gollakota, D. Wetherall, and J. Smith, "Ambient backscatter: Wireless communication out of thin air," in *Proc. ACM SIGCOMM*, Sep. 2013, pp. 39–50.

[6] A. N. Parks, A. Liu, S. Gollakota, and J. R. Smith, "Turbocharging ambient backscatter communication," in *Proc. ACM SIGCOMM*, Aug. 2014, pp. 619–630.

[7] D. Bharadia, K. R. Joshi, M. Kotaru, and S. Katti, "BackFi: High throughput WiFi backscatter," in *Proc. ACM SIGCOMM*, Aug. 2015, pp. 283–296.

[8] D. Li, "Capacity of backscatter communication with frequency shift in Rician fading channels," *IEEE Wireless Commun. Lett.*, vol. 8, no. 6, pp. 1639–1643, 2019.

[9] D. Li, W. Peng, and F. Hu, "Capacity of backscatter communication systems with tag selection," *IEEE Trans. Veh. Technol.*, vol. 68, no. 10, pp. 10 311–10 314, 2019.

[10] W. Zhao, G. Wang, S. Atapattu, C. Tellambura, and H. Guan, "Outage analysis of ambient backscatter communication systems," *IEEE Commun. Lett.*, vol. 22, no. 8, pp. 1736–1739, 2018.

[11] W. Zhao, G. Wang, R. Fan, L. Fan, and S. Atapattu, "Ambient backscatter communication systems: Capacity and outage performance analysis," *IEEE Access*, vol. 6, pp. 22 695–22 704, 2018.

[12] Q. Zhang, H. Guo, Y. Liang, and X. Yuan, "Constellation learning-based signal detection for ambient backscatter communication systems," *IEEE J. Sel. Areas Commun.*, vol. 37, no. 2, pp. 452–463, 2019.

[13] G. Yang, Q. Zhang, and Y. Liang, "Cooperative ambient backscatter communications for green internet-of-things," *IEEE Internet Things J.*, vol. 5, no. 2, pp. 1116–1130, 2018.

[14] H. Guo, Y. Liang, R. Long, and Q. Zhang, "Cooperative ambient backscatter system: A symbiotic radio paradigm for passive IoT," *IEEE Wireless Commun. Lett.*, vol. 8, no. 4, pp. 1191–1194, 2019.

[15] H. Ding, D. B. da Costa, and J. Ge, "Outage analysis for cooperative ambient backscatter systems," *IEEE Wireless Commun. Lett.*, vol. 9, no. 5, pp. 601–605, 2020.

[16] W. Chen, H. Ding, S. Wang, D. B. da Costa, F. Gong, and P. H. J. Nardelli, "Ambient backscatter communications over NOMA downlink channels," *China Communications*, vol. 17, no. 6, pp. 80–100, 2020.

[17] ——, "Backscatter cooperation in NOMA communications systems," *IEEE Trans. Wireless Commun.*, vol. 20, no. 6, pp. 3458–3474, 2021.

[18] Z. Ding, "Harvesting devices heterogeneous energy profiles and QoS requirements in IoT: WPT-NOMA vs BAC-NOMA," *IEEE Trans. Commun.*, vol. 69, no. 5, pp. 2837–2850, May 2021.

[19] Z. Xiang, S. Han, H. Peng, Y. Pei, and Y.-C. Liang, "A cross-layer analysis for symbiotic network using CSMA/CN protocol," *IEEE Internet Things J.*, vol. 8, no. 7, pp. 5697–5709, April 2021.

[20] Y. Guo, G. Wang, R. Xu, R. He, X. Wei, and C. Tellambura, "Capacity analysis for wireless symbiotic communication systems with BPSK tags under sensitivity constraint," *IEEE Commun. Lett.*, vol. 26, no. 1, pp. 14–18, Jan. 2022.

[21] Q. Zhang, Y.-C. Liang, H.-C. Yang, and H. V. Poor, "Mutualistic mechanism in symbiotic radios: When can the primary and secondary transmissions be mutually beneficial?" *IEEE Trans. Wireless Commun.*, Accepted for publication in early access issues.

[22] Q. Zhang, L. Zhang, Y. Liang, and P. Kam, "Backscatter-NOMA: A symbiotic system of cellular and internet-of-things networks," *IEEE Access*, vol. 7, pp. 20 000–20 013, Feb. 2019.

[23] S. Zhou, W. Xu, K. Wang, C. Pan, M.-S. Alouini, and A. Nallanathan, "Ergodic rate analysis of cooperative ambient backscatter communication," *IEEE Wireless Commun. Lett.*, vol. 8, no. 6, pp. 1679–1682, Dec. 2019.

[24] T. Riihonen, S. Werner, and R. Wichman, "Mitigation of loopback self-interference in full-duplex MIMO relays," *IEEE Trans. Signal Processing*, vol. 59, no. 12, pp. 5983–5993, 2011.

[25] H. Hamazumi, K. Imamura, N. Iai, K. Shibuya, and M. Sasaki, "A study of a loop interference canceller for the relay stations in an SFN for digital terrestrial broadcasting," *in Proc. IEEE Global Telecommun. Conf.*, vol. 1, Nov. 2000.

[26] K. M. Nasr, J. P. Cosmas, M. Bard, and J. Gledhill, "Performance of an echo canceller and channel estimator for on-channel repeaters in DVB-T/H networks," *IEEE Trans. Broadcasting*, vol. 53, no. 3, pp. 609–618, Sept. 2007.

[27] G. Kramer, M. Gastpar, and P. Gupta, "Cooperative strategies and capacity theorems for relay networks," *IEEE Trans. Inf. Theory*, vol. 51, no. 9, pp. 3037–3063, Sept. 2005.

[28] T. M. Cover and A. A. E. Gamal, "Capacity theorems for the relay channel," *IEEE Trans. Inf. Theory*, vol. 25, no. 5, pp. 572–584, Sept. 1979.

[29] G. Yang, Y.-C. Liang, R. Zhang, and Y. Pei, "Modulation in the air: Backscatter communication over ambient OFDM carrier," *IEEE Trans. Commun.*, vol. 66, no. 3, pp. 1219–1233, Mar. 2018.

[30] I. S. Gradshteyn and I. M. Ryzhik, *Table of Integrals, Series, and Products, 7th ed.* San Diego, CA: Academic, 2007.

[31] M. Abramowitz and I. A. Stegun, *Handbook of Mathematical Functions with Formulas, Graphs, and Mathematical Tables*. New York, USA: Dover Publications, 1972.

[32] H. Ding, D. B. da Costa, M.-S. Alouini, J. Ge, and F.-K. Gong, "Distributed role selection with ANC and TDBC protocols in two-way relaying systems," *IEEE Trans. Commun.*, vol. 63, no. 12, pp. 4727–4742, Dec. 2015.

[33] H. Ding, D. B. da Costa, H. A. Suraweera, and J. Ge, "Role selection cooperative systems with energy harvesting relays," *IEEE Trans. Wireless Commun.*, vol. 15, no. 6, pp. 4218–4233, Jun. 2016.

[34] H. Ding, J. Ge, D. B. da Costa, and T. Tsiftsis, "A novel distributed antenna selection scheme for fixed-gain amplify-and-forward relaying systems," *IEEE Trans. Veh. Technol.*, vol. 61, no. 6, pp. 2836–2842, July 2012.